Neurobiology of Disease

Reducing $GABA_A$ $\alpha5$ Receptor-Mediated Inhibition Rescues Functional and Neuromorphological Deficits in a Mouse Model of Down Syndrome

Carmen Martínez-Cué,[1] Paula Martínez,[1] Noemí Rueda,[1] Rebeca Vidal,[1,3,4] Susana García,[1] Verónica Vidal,[1] Andrea Corrales,[1] Juan A. Montero,[2] Ángel Pazos,[1,3,4] Jesús Flórez,[1] Rodolfo Gasser,[5] Andrew W. Thomas,[5] Michael Honer,[5] Frédéric Knoflach,[5] Jose Luis Trejo,[6] Joseph G. Wettstein,[5] and Maria-Clemencia Hernández[5]

Departments of [1]Physiology and Pharmacology and [2]Anatomy and Cellular Biology, Faculty of Medicine, University of Cantabria, E-39011 Santander, Spain, [3]Institute of Biomedicine and Biotechnology (University of Cantabria–Spanish National Research Council–Cantabria Research, Development and Innovation), E-39011 Santander, Spain, [4]Center for Biomedical Research Network on Mental Health, Health Institute Carlos III, E-28029 Madrid, Spain, [5]F. Hoffmann-La Roche, Pharma Research and Early Development, Discovery and Translational Area Neuroscience, CH-4070 Basel, Switzerland, and [6]Department of Molecular, Cellular, and Developmental Neurobiology, Cajal Institute, Spanish National Research Council, E-28002 Madrid, Spain

Down syndrome (DS) is associated with neurological complications, including cognitive deficits that lead to impairment in intellectual functioning. Increased GABA-mediated inhibition has been proposed as a mechanism underlying deficient cognition in the Ts65Dn (TS) mouse model of DS. We show that chronic treatment of these mice with RO4938581 (3-bromo-10-(difluoromethyl)-9H-benzo[f]imidazo[1,5-a][1,2,4]triazolo[1,5-d][1,4]diazepine), a selective $GABA_A$ $\alpha5$ negative allosteric modulator (NAM), rescued their deficits in spatial learning and memory, hippocampal synaptic plasticity, and adult neurogenesis. We also show that RO4938581 normalized the high density of GABAergic synapse markers in the molecular layer of the hippocampus of TS mice. In addition, RO4938581 treatment suppressed the hyperactivity observed in TS mice without inducing anxiety or altering their motor abilities. These data demonstrate that reducing GABAergic inhibition with RO4938581 can reverse functional and neuromorphological deficits of TS mice by facilitating brain plasticity and support the potential therapeutic use of selective $GABA_A$ $\alpha5$ NAMs to treat cognitive dysfunction in DS.

Introduction

Down syndrome (DS) is the most common genetic cause of intellectual disability (Bittles et al., 2007). The disorder is caused by trisomy of chromosome 21 and is associated with neurological complications, including cognitive deficits that lead to impairment in intellectual functioning (Lott and Dierssen, 2010). There is currently no pharmacological therapeutic option available for the treatment of cognitive deficits in people with DS.

The genetic dependence of the cognitive phenotype in DS has been recapitulated in mouse models of the condition of which the Ts65Dn (TS) mouse is the most widely used (Kahlem et al., 2004). This murine model shows several fundamental features of DS, including learning and memory deficits (Escorihuela et al., 1995; Reeves et al., 1995; Holtzman et al., 1996) with alterations in both hippocampal morphology (Insausti et al., 1998; Kurt et al., 2004) and adult neurogenesis (Rueda et al., 2005; Clark et al., 2006; Llorens-Martín et al., 2010).

Excessive GABA-mediated neurotransmission has been proposed as one of the underlying causes of the cognitive deficits in TS mice (Belichenko et al., 2004; Fernandez et al., 2007). TS mice display fewer asymmetric synapses that mediate excitatory transmission in the temporal cortex and dentate gyrus (DG) (Kurt et al., 2000, 2004) and synaptic structural abnormalities in the hippocampus and cortex, including a selective reorganization of the inhibitory input (Belichenko et al., 2004; Pérez-Cremades et al., 2010). In addition, enhanced GABA-mediated inhibition was associated with deficient synaptic plasticity in the hippocampus of TS mice through a marked reduction in long-term potentiation (LTP) in the CA1 and DG areas (Siarey et al., 1997; Kleschevnikov et al., 2004; Costa and Grybko, 2005; Fernandez et al., 2007). Furthermore, overexpression of Olig1 and Olig2, two genes triplicated in DS and TS mice, are linked to the neurogenesis defects that led to an imbalance between excitatory and inhibitory neurons and to increased inhibitory drive in the TS forebrain (Chakrabarti et al., 2010). In line with these findings, previous studies showed that reducing inhibitory neurotransmission by chronic administration of nonselective $GABA_A$ receptor antagonists reversed the deficits in LTP and hippocampal-mediated

Received March 9, 2012; revised Dec. 14, 2012; accepted Jan. 3, 2013.

Author contributions: C.M.-C., A.P., J.F., F.K., J.L.T., J.G.W., and M.-C.H. designed research; P.M., N.R., R.V., S.G., V.V., A.C., J.A.M., R.G., A.W.T., and M.H. performed research; C.M.-C., N.R., R.V., V.V., F.K., and M.C.H. analyzed data; C.M.-C. and M.C.H. wrote the paper.

This work was supported by F. Hoffmann-La Roche, the Jerome Lejeune Foundation, and Spanish Ministry of Education and Science Grants BFU2008-04397 and BFU2011-24755. We thank E. García Iglesias, M. Cárcamo, and R. Madureira for their technical assistance, Drs. T. Ballard and G. Trube for helpful discussions, and S. Ortega, S. Gradari, and P. Pérez-Domper for advice on experiments.

R.G., A.W.T., M.H., F.K., J.G.W., and M.-C.H. are employed by F. Hoffmann-La Roche.

This article is freely available online through the *J Neurosci* Open Choice option.

Correspondence should be addressed to Dr. Maria-Clemencia Hernandez, Pharma Research and Early Development, Discovery and Translational Area Neuroscience, F. Hoffmann-La Roche, Grenzacherstrasse 124, CH-4070 Basel, Switzerland. E-mail: maria-clemencia.hernandez@roche.com.

DOI:10.1523/JNEUROSCI.1203-12.2013

 0270-6474/13/333953-14$15.00/0

memory of TS mice (Fernandez et al., 2007; Rueda et al., 2008a). However, nonselective $GABA_A$ receptor antagonists are anxiogenic and proconvulsant (Dorow et al., 1983; Little et al., 1984).

Among the different $GABA_A$ receptor subtypes, $GABA_A$ $\alpha5$ subunit-containing receptors are preferentially localized in the hippocampus and play a key modulatory role in cognition (Collinson et al., 2002; Crestani et al., 2002; Rudolph and Knoflach, 2011). Moreover, selective $GABA_A$ $\alpha5$ negative allosteric modulators (NAMs), also called inverse agonists, have cognition-enhancing effects without anxiogenic or proconvulsant side effects (Collinson et al., 2006; Dawson et al., 2006; Nutt et al., 2007; Ballard et al., 2009). Here we show that RO4938581 (3-bromo-10-(difluoromethyl)-9H-benzo[f]imidazo[1,5-a][1,2,4]triazolo[1,5-d][1,4]diazepine), a selective $GABA_A$ $\alpha5$ NAM, can reverse concomitantly electrophysiological, neuromorphological, and cognitive deficits of TS mice.

Materials and Methods

Animals

This study was approved by the Cantabria University Institutional Laboratory Animal Care and Use Committee and performed in accordance with the Declaration of Helsinki and the European Communities Council Directive (86/609/EEC). For experiments performed at F. Hoffmann-La Roche, the experimental procedures received previous approval from the City of Basel Cantonal Animal Protection Committee based on adherence to federal and local regulations on animal maintenance and testing.

TS mice were generated by repeated backcrossing of B6EiC3Sn a/A-Ts(17<16>)65Dn females with C57BL/6Ei × C3H/HeSNJ (B6EiCSn) F1 hybrid males. The parental generation was provided by the Robertsonian Chromosome Resources (The Jackson Laboratory), and mating was performed at the animal facilities of the University of Cantabria. In all experiments, TS mice were compared with euploid littermates (CO). To determine the presence of the trisomy, animals were karyotyped using real-time quantitative PCR as described previously (Liu et al., 2003). Because C3H/HeSnJ mice carry a recessive mutation that leads to retinal degeneration, all animals were genotyped by standard PCR to screen out all mice carrying this gene.

Mice were housed in groups of two or three in clear Plexiglas cages (20 × 22 × 20 cm) in standard laboratory conditions with a temperature of 22 ± 2°C, 12 h light/dark cycle, and access to food and water *ad libitum*. Light/dark cycle was inverted so that behavioral studies were conducted during the active period of the mice.

In this study, four cohorts of male mice were used. The first cohort was used to determine the effect of RO4938581 on cognition, sensorimotor abilities, and neuromorphology in TS and CO mice, the second cohort was used to test the effects of this compound on anxiety and LTP, the third cohort was used to assess whether or not RO4938581 had a convulsant effect, and the fourth cohort was used for additional LTP studies. All mice were 3–4 months old at the beginning of the treatment. Mice from cohorts one and two received RO4938581 for 6 weeks before the behavioral assessment and for the subsequent behavioral evaluation.

In the first cohort, 10 CO and 10 TS mice received RO4938581; the other two groups of CO ($n = 13$) and TS ($n = 13$) mice received vehicle. In the second cohort, 10 animals per group received RO4938581 or vehicle, and in the third and fourth cohorts, RO4938581 was administered to eight TS and eight CO mice.

Pharmacological treatment

RO4938581 (F. Hoffmann-La Roche) was dissolved in chocolate milk (Puleva) and administered to the mice by voluntary drinking. Before pharmacological treatment, TS and CO mice were conditioned to drink chocolate milk in a clean standard cage from small Petri dishes for 1 week. During the 6 first weeks of drug administration, the mice were introduced individually in clean cages containing a small Petri dish containing either chocolate milk alone (vehicle) or RO4938581 dissolved in chocolate milk (drug) at the same time of the day (10:00 A.M.). Mice drank all the drug or vehicle within 5 min and then were returned to their home cages. The dose of 20 mg/kg RO4938581 in 150 μl of chocolate milk was chosen because it led to plasma concentrations that correlated with 50–70% $GABA_A$ $\alpha5$ receptor occupancy under these conditions. During the behavioral assessment, drug was made available 1 h before testing; all mice regularly consumed the entire chocolate milk–drug mixture. For the study of potential convulsant activity of RO4938581 in TS mice, the compound was prepared in 0.3% Tween 80 v/v 0.9% saline with 100 ml of H_2O and administered orally by gavage (50 mg/kg) to achieve higher plasma and brain exposures.

Behavioral studies

The experimenters were blind to genotype and pharmacological treatment throughout the entire behavioral assessment. Mice from cohort one were used for behavioral testing (actimetry, sensorimotor testing, rotarod, and hole board tests). To decrease the chances of behavioral responses being altered by previous test history, the most invasive procedures were performed last. Studies were performed in the following order: actimetry, sensorimotor testing, rotarod, open field, and hole board. For cohort two, mice were assessed in the plus maze.

Spatial learning and memory: Morris water maze

To evaluate spatial learning and memory, a modified version of the Morris water maze was used. The apparatus was a circular tank 110 cm in diameter, full of water (22–24°C) made opaque by the addition of powdered milk. Inside the tank, a platform was hidden 1 cm below the water level.

Mice were studied at the end of the drug treatment period in 16 consecutive daily sessions: 12 acquisition sessions (platform submerged), followed by a probe trial and four cued sessions (platform visible) (Fig. 1*a*). All trials were videotaped with a camera located 2 m above the water level. The Anymaze computerized tracking system (Stoelting) was used to analyze the mouse trajectories and measure escape latency, distance traveled, swimming speed, and thigmotaxis for each animal in each trial.

We chose this water maze protocol because it allows better observation of the learning deficits of TS mice and, therefore, is more suitable for assessing the efficacy of pharmacological intervention (Stasko and Costa, 2004; Rueda et al., 2008a, b).

Training sessions. In the acquisition sessions (S1–S12), the platform was hidden 1 cm below water level. During the first eight sessions, the platform position was changed every day to assess trial-dependent learning (i.e., spatial working memory). In this protocol, the ability of the animal to find the platform relies only on stochastic search strategy and not an integration of knowledge or memory during the testing or training phases. In sessions 9–12, the platform was placed in the same location (SW) (standard protocol) to assess trial-independent spatial learning. Each of the 12 acquisition and the cued sessions (one session per day) consisted of four pairs of trials, 30–45 min apart. For each trial pair, the mice were randomly started from one of four positions (north, south, east, west), which was held constant for both trials. The first trial of a pair was terminated when the mouse located the platform or when 60 s had elapsed; the second trial commenced after a period of 20 s, during which the mouse was allowed to stay on the platform. Several fixed visual cues outside of the maze were constantly visible from the pool.

Probe trial. After the last acquisition session, a probe trial was performed to evaluate memory of the platform position (spatial memory). During this trial, the platform was removed from the tank. In a single 60 s trial, the number of times that the mice crossed over the place where the platform was located during the acquisition trials, the number of entries in the trained quadrant, and the percentage of time spent in each of the quadrants was recorded.

Cued session. During the cued sessions, the platform was visible: the water level was 1 cm below the platform, and its position was indicated with a flag. Eight trials were performed during each session, following the same experimental procedure as in the acquisition sessions.

Motor tests

Motor coordination and reflex test battery

A battery of motor tests was performed following the procedure described by Rueda et al. (2008b). In the visual placing reflex test, cerebellar and vestibular functions were evaluated. In three consecutive trials, mice

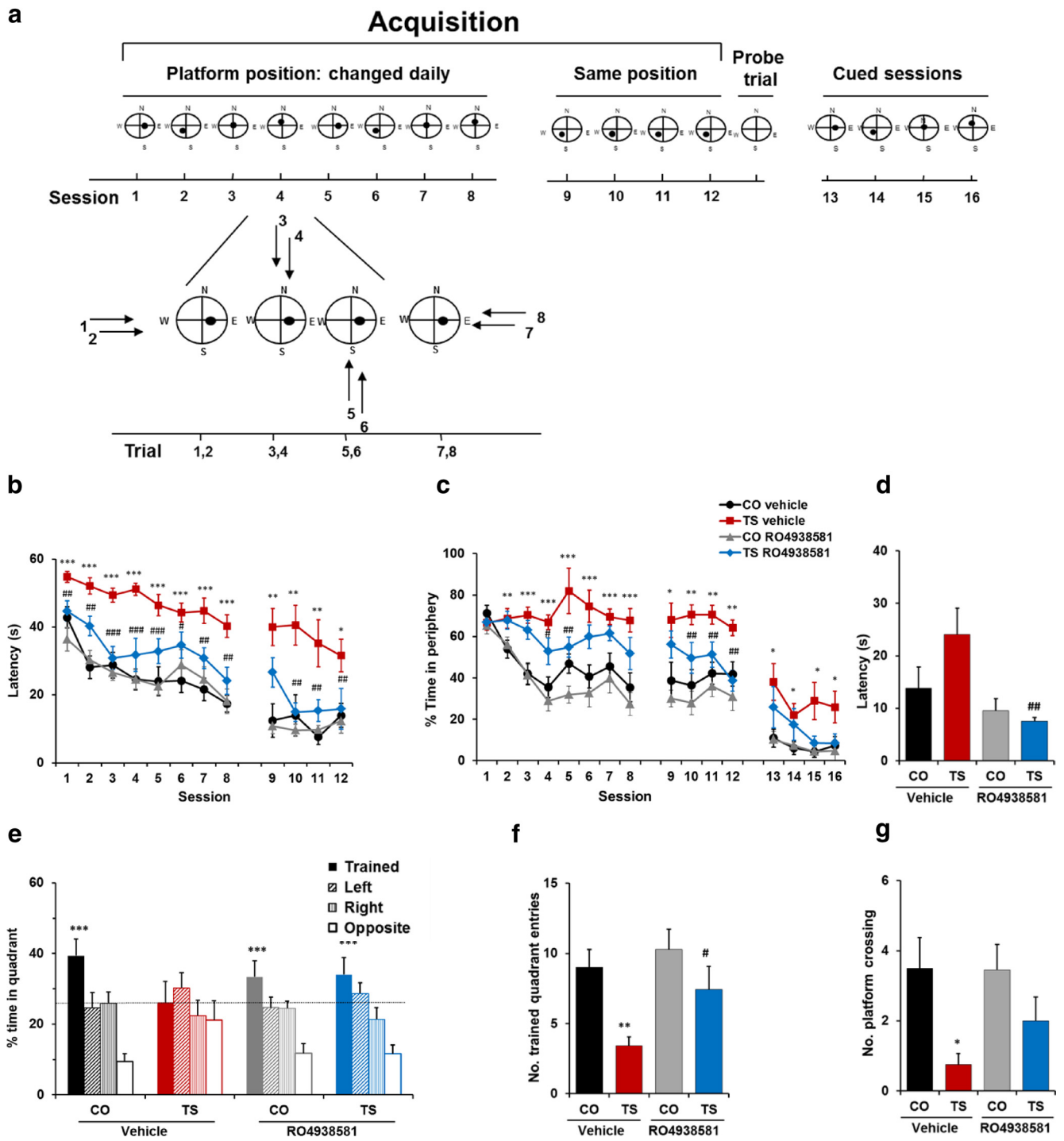

Figure 1. RO4938581 improved spatial learning and memory of TS mice. ***a***, Schematic drawing of the Morris water-maze test design. Chronic treatment with RO4938581 improved performance of TS mice in the acquisition and probe sessions of the Morris water maze. In addition, RO4938581 treatment reduced thigmotactic behavior in TS and CO mice. Data are presented as means ± SEM of the latency to reach the platform during the 12 acquisition (***b***) and cued (***d***) sessions, the percentage of time spent in the periphery of the maze during the acquisition sessions (***c***), the percentage of time in the four quadrants during the probe trial (***e***), the number of entries in the trained quadrant (***f***), and the number of crossings over the platform position (***g***) by the four groups of mice. $^{*}p < 0.05$, $^{**}p < 0.01$, $^{***}p < 0.001$, TS versus CO; $^{\#}p < 0.05$, $^{\#\#}p < 0.01$, $^{\#\#\#}p < 0.001$, vehicle versus RO4938581, Bonferroni's tests after significant ANOVAS (RM-ANOVAs; for statistics, see Table 3).

were gently lowered by the tail toward a flat surface from a height of 15 cm. The response of forepaw extension was scored on a 0–4 scale: 4, animal extends the forepaws when placed at the highest height; 3, forepaws extended before touching the surface with vibrissae; 2, forepaws extended after vibrissae touched the surface; 1, forepaws extended after the nose touched the surface; 0, no extension.

To evaluate auditory sensitivity, the startle response to a sudden auditory stimulus was measured. Mice were placed facing the wall of an unfamiliar cage, and the auditory stimulus was generated by clapping together two stainless steel forceps (7 cm long). A score (0–3 points) was assigned based on the magnitude of the response: 3 points, jumping >1 cm; 2 points, jumping <1 cm; 1 point, retracting of the ears (Preyer reflex); 0 points, no response.

The vibrissa placing reflex was analyzed by noting the reflective reaction to touching the vibrissae with a cotton stick. In three consecutive trials, a score of 1 was assigned to animals that touched the

stimulated vibrissae with an ipsilateral paw and 0 if there was no response.

Grip strength was assessed by quantifying the resistance to being separated from a lid of aluminum bars (2 mm), when dragged by the tail: 0, no resistance, total loss of grip strength; 1, slight; 2, moderate; 3, active; 4, extremely active resistance, normal grip strength.

To evaluate equilibrium, four 20 s trials of balance were performed on an elevated (40 cm high), horizontal (50 cm long) rod. Trials 1 and 2 were performed on a flat wooden rod (9 mm wide); trials 3 and 4 were performed on a cylindrical aluminum rod (1 cm diameter). In each trial, the animals were placed in a marked central zone (10 cm) on the elevated rod. A score of 0 was given if the animal fell within 20 s, 1 if it stayed within the central zone for >20 s, 2 if it left the central zone, and 3 if it reached one of the ends of the bar.

Prehensile reflex (three 5 s trials) was measured as the ability of the animal to remain suspended by the forepaws by grasping an elevated horizontal wire (2 mm in diameter). The maximum possible score of 3 was achieved when the animal remained suspended by the forepaws in all three trials (1 point per trial). Traction capacity was scored at the same time by assessing the number of hindlimbs that the animal raised to reach the wire: 0, none; 1, one limb; 2, two limbs.

Motor coordination: rotarod

Motor coordination was evaluated using a rotarod device (Ugo Basile) that consisted of a 37 cm long, 3 cm diameter plastic rod that rotates at different speeds. In a single session, four trials with a maximum duration of 60 s each were performed. In the first three tests, the rod was rotated at constant speeds of 5, 25, and 50 rpm, respectively. The last trial consisted of an acceleration cycle, in which the rod rotated progressively faster, and the animal had to adapt to the growing demands of the test. The length of time that each animal stayed on the rotarod during the acceleration cycle was recorded.

Spontaneous activity: actimetry

In this test, the circadian variation of the animals' spontaneous locomotor activity during a complete light/dark cycle of 24 h was evaluated. The apparatus is a device (Acti-System II; Panlab) that detects the changes produced in a magnetic field by the movement of the mice. It registers the movements of animals during a continuous 24 h cycle (12 h of light and 12 h of darkness).

Anxiety

Open field

Exploratory behavior and anxiety were assessed using a square-shaped open field (55 × 55 cm, surrounded by a 25-cm-tall fence), divided into 25 equal squares. The mice were placed in the center of the field, and the number of vertical (rearing) activities and horizontal crossings (from square to square, subdivided into center vs peripheral crossings) were scored in a single 5 min trial.

Plus maze

The elevated plus maze consisted of two closed arms (5 × 30 cm, with clear perplex walls 15 cm high) and two open arms (5 cm wide × 30 cm long) raised 40 cm from the floor. In a single 5 min trial, the mice were placed in the center of the maze, and the number of arm entries, the time spent in open and closed arms, and number of stretch attend postures (SAPs) and head dippings (HDs) were registered. Entries to the open arms and time spent and distance traveled in these arms are exploratory behaviors negatively correlated with anxiety. The number of SAPs and HDs constitutes the degree of risk assessment performed by mice and cognitive components of anxiety (Rodgers and Johnson, 1995). The trials were videotaped, and both the distance traveled by each mouse in open and closed arms and the speed in each trial were measured with the computerized tracking system Anymaze.

Exploratory activity: hole board

The hole board is a wooden box (32 × 32 × 30 cm) with four holes. The floor is divided into nine 10 cm squares. In a single 5 min trial, the number of explorations, the time spent exploring each hole, and overall activity in the apparatus were measured. A repetition index was also calculated (exploration of holes explored previously) as a function of the number of A–B–A alternations.

Assessment of possible seizure activity

Potential convulsant effect of RO4938581 at concentrations above efficacious plasma levels was assessed after a single gavage administration of 50 mg/kg of the compound. Each mouse was placed in a transparent box with sawdust bedding in which it could be observed, and the proportion of mice that exhibited tonic convulsions was recorded for 1 h.

In vivo binding of RO4938581 to $GABA_A$ α5 receptors

Tritiated RO0154513 (Ethyl 8-azido-5,6-dihydro-5-methyl-6-oxo-4H-imidazo[1,5-a][1,4]benzodiazepine-3-carboxylate) was synthesized in the isotope laboratory of F. Hoffmann-La Roche with a specific activity of 52 Ci/mmol. Male TS and CO mice (body weights, 20–37 g) were used for the *in vivo* binding experiments. RO4938581 was dissolved in chocolate milk and administered orally at a concentration of 20 mg/kg in a volume of 150 μl. Three CO mice and two TS mice were pretreated with RO4938581 and 60 min later intravenously received 0.1 mCi/kg [^{3}H]RO0154513 (equivalent to a dose of 0.6 μg/kg). Mice were killed by decapitation 15 min after administration of the radioligand. Brains and blood were collected from each mouse. Blood was collected in heparin–lithium tubes (Milian), and all samples were submitted to the Roche analytical laboratories for the determination of RO4938581 exposure. Brains were rapidly removed, divided in two halves along their sagittal axis, and frozen in dry ice. Half brain was submitted to the Roche analytical laboratories for the determination of the brain concentrations of RO4938581. The other half was placed in a cryostat, and sagittal sections (10 μm thickness) were cut (four sections per brain). Brain sections were mounted on Histobond glass slides (Marienfeld Laboratories Glassware), dried at room temperature, and exposed, together with tritium microscales, to tritium-sensitive imaging plates (BAS-TR2025) for 5 d. The imaging plates were scanned in a Fujifilm BAS-5000 high-resolution phosphor imager, and the amount of [^{3}H]RO0154513 bound to the brain regions of interest was quantified with an MCID M2 image analysis system (Imaging Research) and expressed as femtomoles of [^{3}H]RO0154513 per milligram of protein. Inhibition of radioligand binding by RO4938581 in the hippocampus of TS and CO mice was estimated by using the hippocampus/cerebellum ratio as an indication of specific binding. The cerebellum was chosen as a reference region for nonspecific [^{3}H]RO0154513 binding because this region is almost devoid of $GABA_A$ α5 receptors (Fritschy and Mohler, 1995). The receptor blockade (or occupancy) in the hippocampus produced by RO4938581 was calculated according to the following equation: % blockade = $(1 - (\text{Hi/Ce ratio}_{drug}/\text{Hi/Ce ratio}_{vehicle})) \times 100$.

LTP

Mice were decapitated 1 h after the last oral administration, and the brains were rapidly removed. The hippocampi were dissected, and 400 μm slices were cut with a tissue chopper. Slices were allowed to recover for at least 1 h in an interface chamber at room temperature with artificial CSF containing the following (in mM): 120 NaCl, 3.5 KCl, 2.5 $CaCl_2$, 1.3 $MgSO_4$, 1.25 NaH_2PO_4, 26 $NaHCO_3$, and 10 D-glucose (saturated with 95% O_2 and 5% CO_2). Field EPSPs (fEPSPs) were recorded from the CA1 stratum radiatum with a glass micropipette (1–4 MΩ) containing 2 M NaCl and evoked by stimulation of the Schaffer collaterals with insulated bipolar platinum/iridium electrodes >500 μm away from the recording electrode. The stimulus strength was adjusted to evoke fEPSPs equal to 50% of the relative maximum amplitude without superimposed population spike. After stable baseline recordings (100 μs pulse duration, 0.033 Hz), LTP was induced by theta burst stimulation (10 trains of five pulses at 100 Hz and intervals of 200 ms). The duration of the stimulation pulses was doubled during the tetanus. fEPSPs were amplified, bandpass filtered (1 Hz to 1 kHz), and stored in a computer using the Spike 2 program (Cambridge Electronic Design). For the analysis, fEPSP slopes were expressed as a percentage of the baseline values recorded. Results from several slices were expressed as mean ± SEM. The statistical analysis was performed by repeated-measures (RM) multivariate ANOVA

Table 1. Hole-board data (mean scores ± SEM)

	Vehicle		RO4938581		$F_{(1,43)}$		
	CO	TS	CO	TS	Genotype	Treatment	Genotype × treatment
Crossings (*n*)	79.00 ± 5.24	127.15 ± 11.86***	73.27 ± 8.31	106.11 ± 9.80*	18.98, $p = 0.001$	2.07, $p = 0.057$	0.67, $p = 0.41$
Rearings (*n*)	11.54 ± 1.98	13.77 ± 2.55	17.73 ± 3.06	20.67 ± 5.69	0.63, $p = 0.43$	4.05, $p = 0.051$	0.01, $p = 0.91$
Number of HDs	18.15 ± 1.84	22.62 ± 2.21	14.82 ± 2.00	18.22 ± 1.96	3.63, $p = 0.063$	3.51, $p = 0.068$	0.06, $p = 0.79$
Time exploring holes (s)	33.92 ± 6.63	37.88 ± 7.55	30.43 ± 6.83	26.28 ± 4.17	0.00, $p = 0.98$	1.21, $p = 0.27$	0.35, $p = 0.55$
Time exploring holes with objects (s)	18.98 ± 4.72	19.74 ± 5.09	14.99 ± 2.92	14.91 ± 3.13	0.00, $p = 0.93$	1.00, $p = 0.32$	0.00, $p = 0.92$
Time exploring holes without object (s)	14.92 ± 2.77	17.99 ± 3.13	15.44 ± 5.18	11.39 ± 1.94	0.02, $p = 0.88$	0.73, $p = 0.39$	1.00, $p = 0.32$
A–B–A index (*n* of repetitions of recently explored holes)	3.23 ± 0.53	5.23 ± 0.60*	2.64 ± 0.86	3.89 ± 0.72	5.72, $p = 0.021$	2.02, $p = 0.16$	0.30, $p = 0.58$
A–B–A/number of HDs	0.17 ± 0.02	0.24 ± 0.02*	0.15 ± 0.03	0.21 ± 0.02	5.011, $p = 0.031$	0.57, $p = 0.45$	0.04, $p = 0.84$

*$p < 0.05$; ***$p < 0.001$, TS versus CO.

(MANOVA) (time × treatment × genotype). All the analyses were done using SPSS for Windows version 18.0.

Histological and stereological procedures

Mice were deeply anesthetized with pentobarbital and transcardially perfused with saline, followed by 4% paraformaldehyde. After being removed and postfixed in 4% paraformaldehyde overnight at 4°C and transferred into 30% sucrose, the brains were frozen in dry ice and sliced coronally in a cryostat (50-μm-thick sections). Series of brain slices were randomly made up of one section of every eight for the immunohistochemistry protocol.

Granule cell count

One-in-eight series of sections was selected at random and 4′6-diamidino-2-phenylindole (DAPI) stained; for this purpose, mature granule cells in the hippocampal granule cell layer (GCL) were counted in sections stained with DAPI (1:1000;Calbiochem) for 10 min in phosphate buffer (PB) (0.1 M). Cell counts were measured using a previously described physical dissector system coupled to confocal microscopy (Llorens-Martín et al., 2006). Random numbers were generated to select the points where to locate the dissectors. Six dissectors in each section were measured. In the selected points, the confocal microscope was directed toward a position previously established randomly inside the granule layer. Next, in each point, a series of 11 confocal images was serially recorded keeping to the general rules of the physical dissector and the unbiased stereology. The confocal images were then analyzed by the computer with the aid of NIH ImageJ software (version 1.33; http://rsb.info.nih.gov/ij). Every successive pair of images was used, considering one of them the reference image and the other the sample image. Next, the sample image becomes the reference image of the next pair of images, and so on. The cells were counted with NIH ImageJ Cell Counter, labeling in the screen cell by cell the first time they appear in the series of confocal images. The software generates the total number of cells when the dissector brick is completed. For counting the mature granule neurons in the GCL, the dissector frame was a square situated randomly inside the GCL. The number of cells is then referred to the reference volume of the dissector (this parameter is the volume of a prism formed by the area of the frame multiplied by the height of the dissector), to obtain a number of cells per volume unit (cell density).

Cell proliferation in the subgranular zone of the DG (Ki67 immunofluorescence)

Slices were initially preincubated in PB with 1% Triton X-100 and 1% bovine serum albumin (BSA), and then dual immunohistochemistry was performed as described previously (Llorens-Martín et al., 2006). Briefly, free-floating slices were incubated with primary antibody rabbit anti-Ki67 (1:750; Abcam) diluted in PB with 1% Triton X-100 and 1% BSA for 2 d at 4°C. Then slices were incubated overnight at 4°C with secondary antibody Alexa Fluor 594-conjugated donkey anti-rabbit IgG (1:1000; Invitrogen). The sections were counterstained with DAPI and mounted in gelatin-covered slides to be analyzed and photographed. The total number of Ki67-positive cells were counted with the help of an optical fluorescence microscope (Leica DMI 6000 B, oil-immersion 40× objective) using the optical dissector method described previously (Llorens-Martín et al., 2006).

Density of GABAergic synapse markers (glutamate decarboxylases 65 and 67, vesicular GABA transporter, and gephyrin immunofluorescence)

Three dedicated sets of 1-in-8 series of 50 μm sections of mouse brains were used for the determination of GABAergic boutons. GABAergic synapses in the hippocampus were identified by immunocytochemistry with three GABAergic synapse markers mouse anti-glutamate decarboxylase 65 (GAD65, 1:500; Millipore Bioscience Research Reagents), followed by Alexa Fluor 594-conjugated donkey anti-mouse Ig (1:1000; Invitrogen), rabbit anti-glutamate decarboxylase 67 (GAD67, 1:200; Abcam), and rabbit anti-vesicular GABA transporter (VGAT, 1:200; Millipore Bioscience Research Reagents), followed by Alexa Fluor 488 donkey anti-rabbit Ig (1:1000; Invitrogen). To study colocalization of VGAT with the postsynaptic scaffolding protein marker gephyrin, slices were submitted to double-labeling immunohistochemistry anti-VGAT (1:200; Millipore Bioscience Research Reagents), followed by Alexa Fluor 488 donkey anti-rabbit Ig (1:1000; Invitrogen) and anti-gephyrin (1:200; Synaptic Systems), followed by Alexa Fluor 594-conjugated donkey anti-mouse Ig (1:1000; Invitrogen). Measurements were performed in images recorded with a confocal microscope (Leica TCS 4D), using a 63× oil objective and a 9× zoom. For each synapse marker, four sections per animal were used comprising the entire hippocampus, and one random area in the hippocampus per section was measured. Image analysis was performed with the aid of NIH ImageJ software (version 1.33; http://rsb.info.nih.gov/ij). Briefly, boutons with positive immunofluorescence (GAD65, GAD67, VGAT, or gephyrin) were measured separately applying the same threshold to all pictures. Images were previously converted to grayscale to improve the contrast between signal and noise. Areas were measured inside a reference circle with a standard size of 325 μm^2. Reference space was located in the inner molecular layer of the hippocampal DG, lining the most external layer of granule neurons in the GCL. The percentage of reference area occupied by GAD65-, GAD67-, VGAT-, gephyrin-, and VGAT/gephyrin-positive boutons was calculated.

Statistical analyses

The water maze data of the acquisition sessions (S1–S8 and S9–S12) and thigmotactic behavior were analyzed using a two-way RM-ANOVA (session × genotype × treatment or trial × genotype × treatment). LTP data were analyzed by RM-MANOVA (time × treatment × genotype). The rest of the behavioral and neuromorphological data were analyzed using two-way (genotype × treatment) ANOVAs. The means of each experimental group were compared *post hoc* by Student's *t* test if two groups were compared or Bonferroni's tests if more than two groups were compared. All the analyses were done using SPSS for Windows version 18.0. The *F* values of RM-ANOVAs, two-way ANOVAs, and *post hoc* analysis of each independent variable tested in the Morris water maze, LTP, hole board, sensorimotor abilities, open field, and plus maze and are shown in Tables 1–5, respectively.

Table 2. Sensorimotor test battery, rotarod, and actimetry (mean scores ± SEM)

	Vehicle		R04938581		$F_{(1,43)}$		
	CO	TS	CO	TS	Genotype	Treatment	Genotype × treatment
Vision (score 0–4 × 3 trials)	8.54 ± 0.57	8.23 ± 0.60	7.64 ± 0.47	7.67 ± 0.88	0.07, $p = 0.79$	1.18 $p = 0.28$	0.09, $p = 0.75$
Auditory startle (score 0–3)	1.31 ± 0.24	1.15 ± 0.19	1.00 ± 0.13	1.33 ± 0.17	0.22, $p = 0.63$	0.12, $p = 0.72$	1.38, $p = 0.24$
Righting reflex (score 0–3)	3.00 ± 0.00	3.00 ± 0.00	3.00 ± 0.00	3.00 ± 0.00			
Grip strength (score 0–3)	2.00 ± 0.28	1.62 ± 0.24	1.55 ± 0.21	2.00 ± 0.24	0.00, $p = 0.92$	0.00, $p = 0.92$	3.71, $p = 0.061$
Latency to fall wooden bar (s)	19.8 ± 0.19	20.0 ± 0.0	20.00 ± 0.00	20.00 ± 0.00	0.75, $p = 0.38$	0.75, $p = 0.38$	0.75, $p = 0.38$
Equilibrium aluminum bar							
(score 1–3)	1.38 ± 0.43	2.31 ± 0.54	1.36 ± 0.45	1.00 ± 0.44	0.18, $p = 0.67$	1.48, $p = 0.23$	1.38, $p = 0.24$
Latency to fall aluminum bar (s)	14.03 ± 1.42	15.11 ± 1.55	14.73 ± 1.28	12.11 ± 2.07	0.37, $p = 0.54$	0.35, $p = 0.55$	1.05, $p = 0.31$
Prehensile reflex (score 0–3)	2.69 ± 0.17	2.92 ± 0.83	2.45 ± 0.31	2.67 ± 0.24	1.05, $p = 0.31$	1.31, $p = 0.25$	0.00, $p = 0.97$
Traction capacity (score 0–3)	2.31 ± 0.63	2.67 ± 0.62	1.82 ± 0.55	1.67 ± 0.62	0.02, $p = 0.86$	1.43, $p = 0.23$	0.16, $p = 0.68$
Number of crossings coat hanging	3.62 ± 0.96	3.67 ± 0.34	2.64 ± 0.43	3.33 ± 0.50	1.46, $p = 0.23$	2.56, $p = 0.11$	1.29, $p = 0.26$
Latency arrival coat hanging (s)	36.00 ± 5.62	32.42 ± 6.16	46.45 ± 5.79	35.44 ± 5.76	1.54, $p = 0.22$	1.28, $p = 0.26$	0.39, $p = 0.53$
Rotarod (latency to fall, s)							
5 rpm	60.00 ± 0.00	60.00 ± 0.00	60.00 ± 0.00	60.00 ± 0.00			
25 rpm	30.38 ± 5.85	39.92 ± 6.42	35.63 ± 7.47	34.33 ± 6.87	0.37, $p = 0.54$	0.00, $p = 0.98$	0.65, $p = 0.42$
50 rpm	11.53 ± 3.67	11.76 ± 4.24	16.27 ± 3.99	10.22 ± 3.79	0.51, $p = 0.47$	1.55, $p = 0.69$	0.60, $p = 0.44$
Acceleration cycle	126.53 ± 15.55	158.38 ± 19.73	146.0 ± 17.56	145.55 ± 29.50	0.59, $p = 0.44$	0.02, $p = 0.87$	0.63, $p = 0.43$
Actimetry (counts)							
Dark	107030.7 ± 18863.97	90334 ± 4202.28	90334.4 ± 21059.53	85212.86 ± 10008.14	1.16, $p = 0.28$	0.28, $p = 0.59$	0.83, $p = 0.36$
Light	19014.79 ± 4144.34	17850.61 ± 4202.28	21653.61 ± 2096.76	7732.37 ± 2048.73	0.52, $p = 0.47$	0.34, $p = 0.56$	0.07, $p = 0.78$

Table 3. *F* values of RM-MANOVAs and *post hoc* analysis of each independent variable tested in the acquisition and cued sessions of the Morris water maze

	Session	Genotype	Treatment	Genotype × treatment
Acquisition between sessions (S1–S8)				
RM-MANOVA genotype × treatment	$F_{(7,38)} = 18.71, p < 0.001$	$F_{(1,38)} = 26.91, p < 0.001$	$F_{(1,38)} = 10.68, p = 0.002$	$F_{(1,38)} = 10.83, p = 0.002$
Post hoc comparisons between each pair of learning curves				
Vehicle CO versus vehicle TS		$F_{(1,23)} = 46.14, p < 0.001$		
RO4938581 CO versus RO4938581 TS		$F_{(1,18)} = 1.49, p = 0.24$		
Vehicle TS versus RO4938581 TS			$F_{(1,23)} = 31.33, p < 0.001$	
Vehicle CO versus RO4938581 CO				$F_{(1,22)} = 0.00, p = 0.98$
Acquisition (S9–S12)				
RM-MANOVA genotype × treatment	$F_{(3,38)} = 11.56, p = 0.002$	$F_{(1,38)} = 16.24, p < 0.001$	$F_{(1,38)} = 6.11, p = 0.020$	$F_{(1,38)} = 8.19, p = 0.008$
Post hoc comparisons between each pair of learning curves				
Vehicle CO versus vehicle TS		$F_{(1,23)} = 15.04, p = 0.002$		
RO4938581 CO versus RO4938581 TS		$F_{(1,18)} = 1.98, p = 0.18$		
Vehicle TS versus RO4938581 TS			$F_{(1,23)} = 7.65, p = 0.018$	
Vehicle CO versus RO4938581 CO				$F_{(1,22)} = 0.16, p = 0.69$
Acquisition between trials				
RM-MANOVA genotype × trial	Trial: $F_{(7,38)} = 6.04, p < 0.001$	$F_{(1,42)} = 35.62, p < 0.001$	$F_{(1,38)} = 14.59, p < 0.001$	$F = 14.78, p < 0.001$
Post hoc comparisons between each pair of learning curves				
Vehicle CO versus vehicle TS		$F_{(1,23)} = 50.67, p < 0.001$		
RO4938581 CO versus RO4938581 TS		$F_{(1,18)} = 2.28, p = 0.14$		
Vehicle TS versus RO4938581 TS			$F_{(1,23)} = 49.42, p < 0.001$	
Vehicle CO versus RO4938581 CO				$F_{(1,22)} = 0.00, p = 0.99$
Thigmotaxis				
(All sessions) RM-MANOVA genotype × treatment	$F_{(11,38)} = 13.92, p < 0.001$	$F_{(1,38)} = 20.73, p < 0.001$	$F_{(1,38)} = 7.82, p = 0.009$	$F_{(1,38)} = 1.89, p = 0.18$
S1–S12 *post hoc* comparisons RM-MANOVA session × group				
TS vehicle: $F_{(11,9)} = 1.09, p = 0.37$				
CO vehicle: $F_{(11,9)} = 6.43, p < 0.001$				
TS RO4938581: $F_{(11,12)} = 5.62, p < 0.001$				
CO RO4938581: $F_{(11,12)} = 10.09, p < 0.001$				
Mean of cued sessions MANOVA genotype × treatment		$F_{(1,38)} = 9.82, p = 0.004$	$F_{(1,38)} = 2.43, p = 0.13$	$F_{(1,38)} = 2.14, p = 0.15$
Probe trial				
n of crossings over platform				
MANOVA genotype × treatment		$F_{(1,38)} = 9.27, p = 0.005$	$F_{(1,38)} = 1.21, p = 0.29$	$F_{(1,38)} = 0.43, p = 0.51$
n of entries in trained quadrant				
MANOVA genotype × treatment		$F_{(1,38)} = 10.41, p = 0.003$	$F_{(1,38)} = 5.24, p = 0.030$	$F_{(1,38)} = 0.69, p = 0.41$
Percentage of time in quadrants				
MANOVA quadrant × genotype × treatment	Quadrant: $F_{(3,37)} = 13.56, p = 0.001$	$F_{(1,38)} = 2.91, p = 0.021$	$F_{(1,38)} = 10.92, p = 0.002$	$F_{(1,38)} = 1.10, p = 0.30$
Cues sessions				
Latency				
MANOVA genotype × treatment:treatment		$F_{(1,38)} = 3.93, p = 0.054$	$F_{(1,38)} = 8.58, p = 0.006$	$F_{(1,38)} = 5.76, p = 0.021$
Speed				
MANOVA genotype × treatment		$F_{(1,38)} = 2.77, p = 0.10$	$F_{(1,38)} = 0.55, p = 0.46$	$F_{(1,38)} = 0.011, p = 0.91$

Table 4. *F* values of RM-MANOVA and *post hoc* analysis of potentiation curves for LTP results

	Genotype	Treatment	Genotype × treatment
Basal	$F_{(1,38)} = 0.0.18, p = 0.66$	$F_{(1,38)} = 0.12, p = 0.72$	$F_{(1,38)} = 0.05, p = 0.81$
After theta burst stimulation			
All groups, MANOVA genotype × treatment	$F_{(1,38)} = 0.9.93, p = 0.003$	$F_{(1,38)} = 14.38, p = 0.001$	$F_{(1,38)} = 2.65, p = 0.11$
Post hoc comparisons between each pair of potentiation curves			
Vehicle CO versus vehicle TS	$F_{(1,21)} = 16.05, p = 0.001$		
RO4938581 CO versus RO4938581 TS	$F_{(1,17)} = 0.83, p = 0.37$		
Vehicle TS versus RO4938581 TS		$F_{(1,20)} = 37.73, p < 0.001$	
Vehicle CO versus RO4938581 CO		$F_{(1,18)} = 1.34, p = 0.26$	
Vehicle CO versus RO4938581 TS			$F_{(1,19)} = 0.19, p = 0.66$

Table 5. *F* values of MANOVA (genotype × treatment) for each dependent variable in the open field and plus maze

	Genotype	Treatment	Genotype × treatment
Open field			
Crossings periphery	$F_{(1,43)} = 10.51, p = 0.002$	$F_{(1,43)} = 0.29, p = 0.58$	$F_{(1,43)} = 2.05, p = 0.15$
Crossings center	$F_{(1,43)} = 2.6, p = 0.11$	$F_{(1,43)} = 4.25, p = 0.045$	$F_{(1,43)} = 0.14, p = 0.71$
Total crossings	$F_{(1,43)} = 12.19, p = 0.001$	$F_{(1,43)} = 1.67, p = 0.02$	$F_{(1,43)} = 1.98, p = 0.16$
Rearings	$F_{(1,43)} = 1.63, p = 2.08$	$F_{(1,43)} = 2.89, p = 0.096$	$F_{(1,43)} = 1.97, p = 0.16$
Plus maze			
n of entries open arms	$F_{(1,37)} = 8.33, p = 0.007$	$F_{(1,37)} = 1.20, p = 0.28$	$F_{(1,37)} = 4.32, p = 0.045$
n of entries closed arms	$F_{(1,37)} = 4.96, p = 0.033$	$F_{(1,37)} = 2.04, p = 0.15,$	$F_{(1,37)} = 0.24, p = 0.62$
Total *n* of entries	$F_{(1,37)} = 9.13, p = 0.005$	$F_{(1,37)} = 3.60, p = 0.066$	$F_{(1,37)} = 1.34, p = 0.25$
Initial freezing	$F_{(1,37)} = 0.55, p = 0.46$	$F_{(1,37)} = 1.94, p = 0.17$	$F_{(1,37)} = 0.04, p = 0.83$
Percentage of time in open arms	$F_{(1,37)} = 0.00, p = 0.97$	$F_{(1,37)} = 0.00, p = 0.93$	$F_{(1,37)} = 0.00, p = 0.94$
Risk assessment (SAP + HD)	$F_{(1,37)} = 0.07, p = 0.78$	$F_{(1,37)} = 6.36, p = 0.017$	$F_{(1,37)} = 0.00, p = 0.99$

Results

RO4938581 improved cognition and rescued deficient hippocampal LTP in TS mice

We reported previously that RO4938581 has cognition-enhancing effects in rat and monkey (Ballard et al., 2009). To test whether RO4938581, through inhibition of the $GABA_A$ α5 receptor activity, could improve cognition in TS mice, we used a modified version of the Morris water maze task (Morris et al., 1982) as illustrated in Figure 1*a*. This method allows assessment of working memory (S1–S8, trial-dependent learning), spatial learning (S9–S12, trial-independent learning), and memory (probe trail), all of which are dependent on hippocampal function, followed by four cued trials. Consistent with previous studies, TS mice showed a pronounced learning deficit in the water maze, both during the acquisition sessions in which the platform was placed in different positions and those in which the platform position was kept constant ($p < 0.001$; Fig. 1*a*,*b*). The difference between TS and CO mice learning curves was significantly reduced after chronic treatment with RO4938581 in S1–S8 ($p = 0.24$; Fig. 1*b*) and S9–S12 ($p = 0.21$; Fig. 1*b*). RO4938581 treatment significantly improved the performance of TS mice during the acquisition sessions (S1–S8, $p < 0.001$; S9–S12, $p = 0.005$ Fig. 1*b*) and had no effect on CO mice performance (S1–S8, $p = 0.98$; S9–S12, $p = 0.91$; Fig. 1*b*). During the cued sessions (Fig. 1*d*), RO4938581 treatment also reduced the latency to reach the platform by TS mice ($p = 0.006$). In addition, RO4938581 significantly reduced thigmotactic behavior in TS and CO mice (Fig. 1*c*) because RO4938581-treated TS and CO mice spent significantly less time swimming in the periphery of the maze throughout the acquisition and cued sessions than the corresponding vehicle-treated mice (Fig. 1*c*). The *post hoc* analysis of each of the thigmotactic behavior curves revealed that RO4938581-treated TS and CO mice as well as vehicle-treated CO mice significantly reduced thigmotactic behavior throughout the sessions ($p < 0.001$). In contrast, vehicle-treated TS mice did not reduce the time spent in the periphery of the pool throughout the sessions ($p = 0.37$).

When the performance of the different group of mice was analyzed within sessions (i.e., the latency to reach the platform in each trial across the eight sessions), statistical analysis revealed that vehicle-treated TS mice did not learn to localize the platform position ($p = 0.59$; data not shown) but that all the other groups of mice reduced the latency to reach the platform throughout the trials across sessions ($p = 0.006$), i.e., they learned in each session the new platform position.

During the probe trial, vehicle-treated TS mice showed impaired spatial memory because they did not show any preference for the trained quadrant (i.e., they spent ~25% of the time in each of the quadrants; Fig. 1*e*), had fewer crossings over the place where the platform was located during the acquisition trials (Fig. 1*g*), and entered fewer times in the trained quadrant (Fig. 1*f*). In contrast, RO4938581-treated TS mice spent significantly more time in the trained quadrant (Fig. 1*e*), entered significantly more times in this quadrant (Fig. 1*f*), and crossed more times over the platform position compared with vehicle-treated mice (although this later effect did not reach statistical significance; Fig. 1*g*), indicating that RO4938581 improved the spatial memory impairment of TS mice.

No significant differences were found in the swimming speed of the four groups of mice (data not shown; ANOVA, genotype, $F_{(1,43)} = 0.10$; treatment, $F_{(1,43)} = 0.55$, $p = 0.46$; genotype × treatment, $F_{(1,43)} = 0.01, p = 0.91$). Mean plasma concentrations of RO4938581 determined in a subset of TS and CO animals during chronic treatment were 1815 and 1117 ng/ml, respectively. These plasma concentrations correlate to >50% $GABA_A$ α5 receptor occupancy (see *in vivo* binding results).

To assess the effect of RO4938581 chronic treatment on the hippocampal synaptic transmission and plasticity, we recorded fEPSPs from hippocampal slices of CO and TS mice that were chronically treated with vehicle or RO4938581. A theta burst stimulus was used to induce LTP at the Schaffer collateral–CA1 pathway. No significant differences were found in fEPSP amplitudes in the baseline of the four groups of mice (Table 4). Vehicle-

treated TS mice presented deficits in LTP relative to vehicle-treated CO mice ($p = 0.001$; Fig. 2). In TS mice, RO4938581 treatment produced a marked enhancement of LTP relative to vehicle treatment ($p < 0.001$; Fig. 2). There was a trend ($p = 0.26$) for RO4938581 chronic treatment to facilitate LTP in CO mice (Fig. 2). The amount of LTP measured in RO4938581-treated TS mice was not different from that of vehicle-treated CO mice ($p = 0.66$; Fig. 2). Subsequently, no differences were found between the LTP of RO4938581-treated TS and CO mice ($p = 0.37$ Fig. 2). The relative potentiations at 80 min after tetanus were 165 ± 9% ($n = 11$ slices from 11 different mice), 128 ± 4% ($n = 12$ slices from 12 different mice), 173 ± 16% ($n = 9$ slices from 9 different mice), and 163 ± 12% ($n = 10$ slices from 10 different mice) in vehicle-treated CO and TS and RO4938581-treated CO and TS mice, respectively. These findings confirm the previously reported LTP deficits observed in slices of TS mice (Costa and Grybko, 2005) and demonstrate that chronic treatment with this selective $GABA_A$ α5 NAM can completely rescue LTP in TS mice.

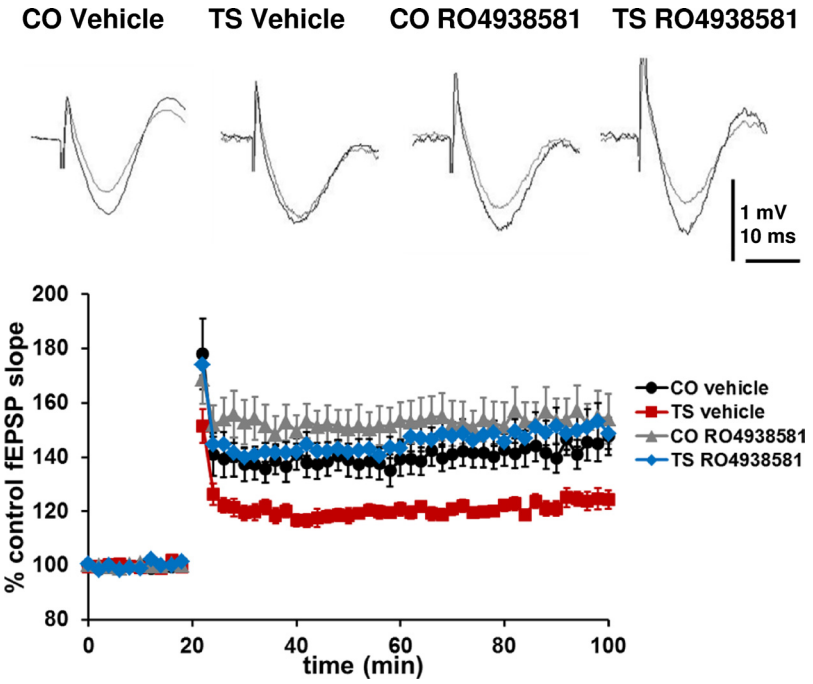

Figure 2. RO4938581 rescued LTP in TS mice. Time courses of the initial slope of fEPSPs recorded from the apical dendritic layer of the CA1 region in hippocampal slices after stimulation of the Schaffer collateral– commissural pathway at 30 s intervals. After 20 min of stable baseline recording, a theta burst stimulus induced robust LTP in hippocampal slices of vehicle-treated CO but not TS mice. Long-term treatment with RO4938581 resulted in enhanced LTP that reached statistical significance in slices of TS but not CO mice. The traces on top are superimposed, representative fEPSPs recorded before issuing the stimulus and at 60 min after stimulation for each genotype. Calibration: 10 ms, 1.0 mV. Data are presented as means ± SEM from vehicle-treated CO ($n = 11$ slices from 11different mice), vehicle-treated TS ($n = 12$ slices from 12 different mice), RO4938581-treated CO ($n = 9$ slices from 9 different mice), and RO4938581-treated TS ($n = 10$ slices from 10 different mice) mice, respectively (for statistics, see Table 4).

RO4938581 rescued deficient neurogenesis and normalized the density of GABAergic synapse markers in the hippocampus of TS mice

Because impairment in hippocampal cell proliferation and neurogenesis is a major pathological hallmark in DS and TS mice, we first assessed whether cell proliferation in the DG was affected by chronic treatment of RO4938581 in TS and CO mice. We used Ki67 immunohistochemistry to estimate the total number of the actively dividing cells and confirmed the reduced number of Ki67-positive cells in the DG of vehicle-treated TS compared with vehicle-treated CO mice ($p = 0.024$). We found that RO4938581 treatment completely restored the number of Ki67-positive cells in the DG of TS mice and produced a less pronounced enhancement in the density of this cell population in CO mice ($p = 0.033$; Fig. 3). In addition, neuronal survival of the cells that have undergone maturation was also normalized in TS mice, as shown by the increase in DAPI-positive cells found in TS hippocampus after chronic RO4938581 administration ($p = 0.045$; Fig. 4). There was no significant increase in DAPI-positive cells in RO4938581-treated CO mice.

Next, we used GAD65, GAD67, and VGAT/gephyrin immunostainings to evaluate whether RO4938581 chronic treatment affected the density of GABAergic synapse markers in the hippocampus of TS and CO mice. We found increased percentage of area occupied by GAD65-, GAD67-, VGAT-, and VGAT/gephyrin-positive boutons in the inner molecular layer of the hippocampal DG of vehicle-treated TS mice compared with vehicle-treated CO mice ($p = 0.001$, $p = 0.001$, $p = 0.001$, and $p = 0.013$ respectively; Fig. 5). After chronic treatment with RO4938581, the percentage of area occupied by GAD65-, GAD67-, VGAT-, and VGAT/gephyrin-positive boutons was significantly decreased in the hippocampus of TS mice similar to that observed in vehicle-treated CO mice ($p = 0.017$, $p = 0.016$, $p = 0.019$, and 0.008 respectively; Fig. 5). RO4938581 treatment produced a nonsignificant tendency to increase the number of GAD65-positive boutons in CO mice ($p = 0.24$). These results indicate that negative modulation at $GABA_A$ α5 receptors by RO4938581 can restore both deficient neurogenesis and enhanced density of GABAergic synapse markers in the hippocampus of TS mice.

RO4938581 improved TS mice attention and did not affect spontaneous activity or motor coordination

In the hole board, TS mice, under both treatments, performed a larger number of crossings than CO mice ($p = 0.001$; Table 1). TS mice showed altered attention because they repeated a larger number of times the exploration of recently explored holes (A–B–A index, $p = 0.021$). After RO4938581 treatment, TS mice A–B–A index was normalized. RO4938581 reduced this activity in mice of both genotypes but this reduction did not reach statistical significance ($p = 0.057$). TS mice also showed a nonsignificant increased number of explorations ($p = 0.063$) that was reduced after RO4938581 ($p = 0.068$). No significant differences were found between mice of both genotypes and treatments in the time they spent exploring the holes.

RO4938581 did not modify any of the sensorimotor abilities tested in neither TS nor CO mice (vision, audition, strength, equilibrium prehensile reflex, traction capacity, or motor coordination in the coat-hanging test). Table 2 shows the score of RO4938581- and vehicle-treated TS and CO mice in the different sensorimotor methods; motor coordination in the rotarod was not affected by genotype or treatment. TS and CO mice presented a similar latency to fall from the rotarod at different constant speeds. Furthermore, no differences were found between RO4938581- and vehicle-treated TS

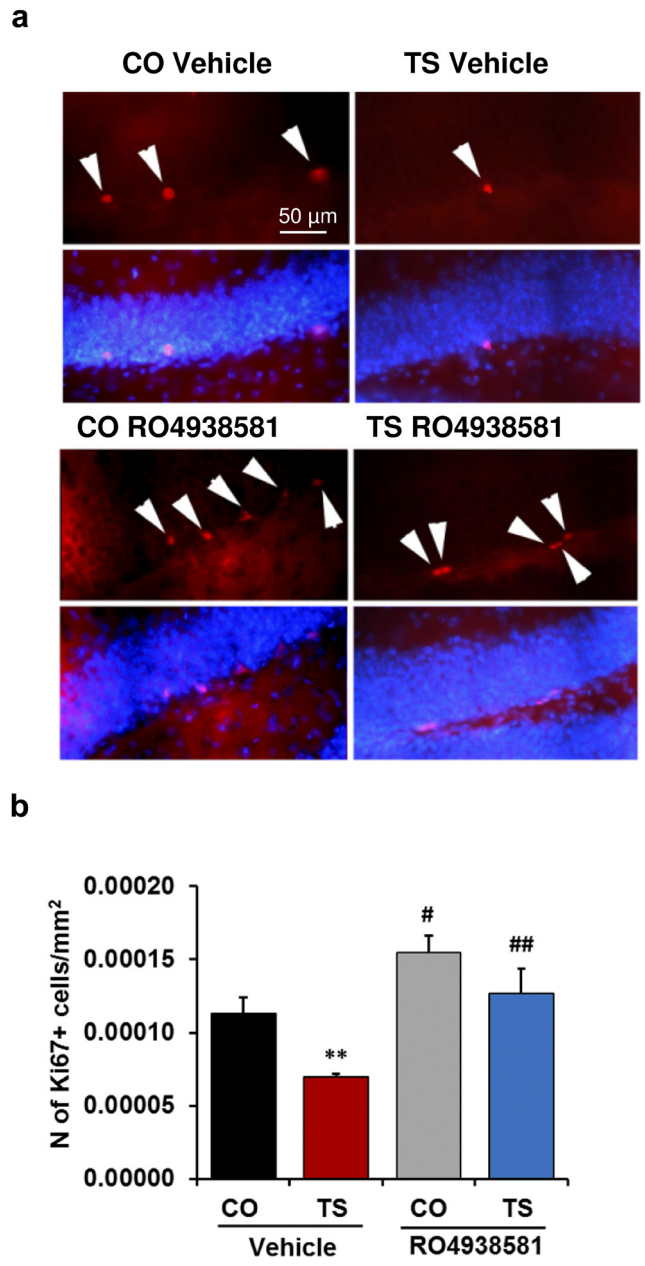

Figure 3. RO4938581 rescued neuronal proliferation in the hippocampus of TS mice. ***a***, Representative microscope images of coimmunostaining of DAPI (labeling all cell nuclei) and Ki-67 (proliferating cells) in the DG region of hippocampus of vehicle- and RO4938581-treated TS and CO mice. Arrowheads indicate Ki-67-positive cells. Scale bar, 50 μm. ***b***, Means ± SEM of the density of Ki67-positive cells in vehicle- and RO4938581-treated TS and CO mice. $^{**}p < 0.01$ TS versus CO; $^{\#}p < 0.05$, $^{\#\#}p < 0.01$ vehicle- versus RO4938581-treated mice; Bonferroni's tests after significant ANOVAs.

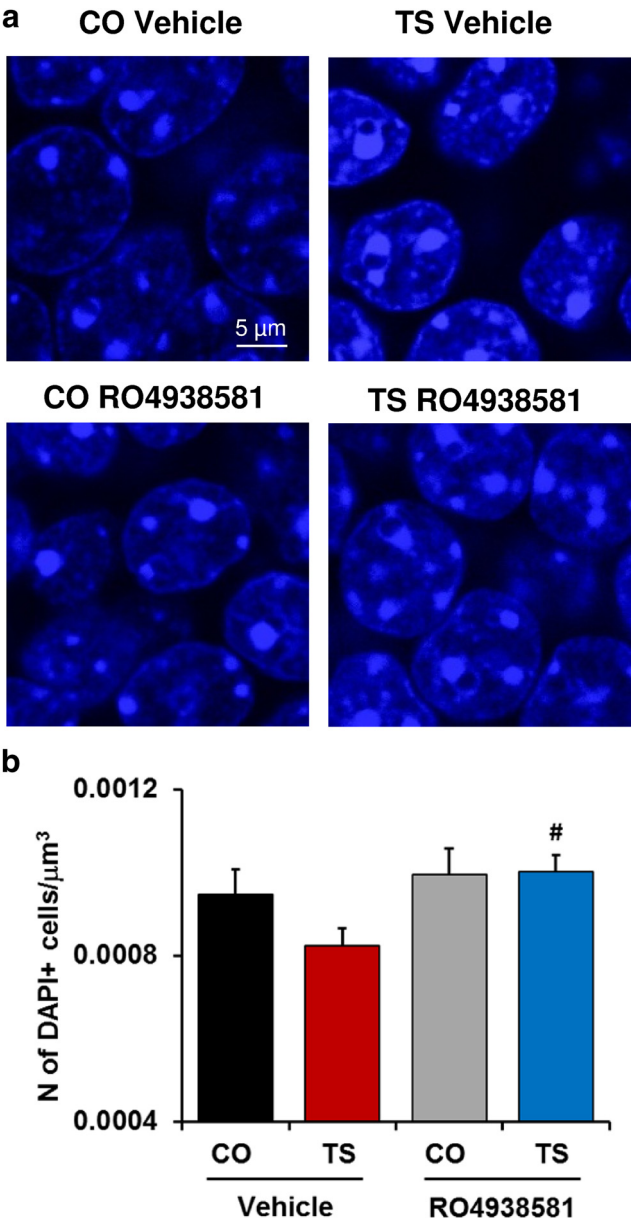

Figure 4. RO4938581 rescued granular cell density in the hippocampus of TS mice. ***a***, Representative microscope images of DAPI immunostaining in the GCL of the hippocampal DG of vehicle- and RO4938581-treated TS and CO mice. Scale bar, 5 μm. ***b***, Means ± SEM of the density of DAPI-positive cells in the GCL of vehicle- and RO4938581-treated TS and CO mice (***a***). $^{\#}p < 0.05$ vehicle- versus RO4938581-treated mice; Bonferroni's tests after significant ANOVAs.

or CO mice in the latency to fall at the different constant speeds. TS and CO mice under both treatments did not differ in the amount of spontaneous activity performed in their home cage during the dark or the light phase of the cycle.

RO4938581 reduced hyperactivity without inducing anxiety-like behavior or convulsions in TS mice

In the open-field test (Fig. 6), both mouse genotypes exhibited similar activity as measured by crossing in the maze center. However, in the peripheral part of the open field, vehicle-treated TS mice showed higher activity than CO mice ($p = 0.002$), which accounted for the increased total activity shown by TS mice ($p = 0.001$). RO4938581 increased the number of crossings performed by CO mice in the center of the open field ($p = 0.045$). Because lower activity in the center of the open field is considered an index of anxiety, an increase in the number of crossings performed by CO mice after RO4938581 treatment suggests that this compound might have mild anxiolytic properties. RO4938581 did not affect general activity in TS and CO mice as indicated by their similar horizontal total number of crossings ($p = 0.20$) and vertical activity ($p = 0.096$; data not shown).

In the plus maze, TS mice were hyperactive because they performed a larger number of entries in the open and closed arms and total number of entries ($p = 0.005$; Fig. 7*a*). Chronic administration of RO4938581 did not affect activity in this procedure

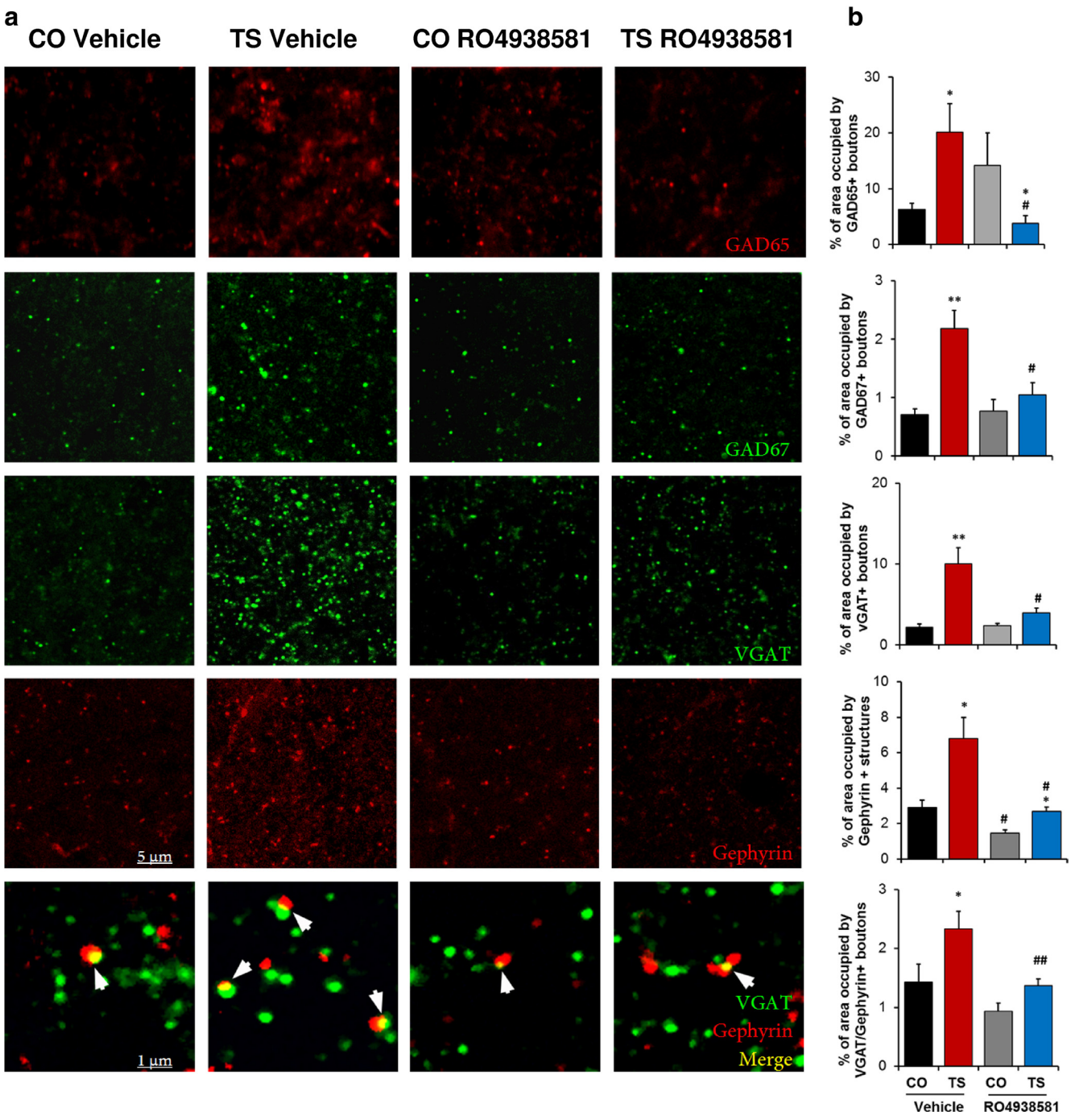

Figure 5. RO4938581 normalized the density of GABAergic synapse markers in the hippocampus of TS mice. ***a***, Representative confocal microscope images of GAD65, GAD67, VGAT, and gephyrin immunostaining in the inner molecular layer of the hippocampal DG, lining the most external layer of granule neuron in the GCL of vehicle- and RO4938581-treated TS and CO mice. ***b***, Means ± SEM of the percentage area occupied by GAD65-, GAD67-, VGAT-, and gephyrin-positive boutons in the hippocampus of vehicle- and RO4938581-treated TS and CO mice. $^{*}p < 0.05$, $^{**}p < 0.01$, TS versus CO; $^{\#}p < 0.05$, $^{\#\#}p < 0.01$, vehicle- versus RO4938581-treated mice; Bonferroni's tests after significant ANOVAs.

($p = 0.066$). Statistical analysis revealed that RO4938581 did not affect the motor components of anxiety because TS and CO mice under the different treatment conditions did not differ in the time freezing at the start of the test ($p = 0.17$; Fig. 7*b*) or in the percentage of time spent in the open arms ($p = 0.93$; Fig. 7*c*). However, RO4938581 reduced the cognitive components of anxiety as indicated by the lower number of risk assessment behaviors performed by TS and CO mice under chronic treatment with this compound ($p = 0.017$; Fig. 7*d*).

We demonstrated previously that RO4938581 lacked convulsant and proconvulsant activity after an auditory stimulus in the DBA/2J mice. In the current study, we tested the convulsant potential of RO4938581 in TS mice after a single oral administration of 50 mg/kg. RO4938581 did not induce convulsions in any of the 16 (eight TS and eight CO) mice tested at mean plasma concentrations of 3720 ng/ml. These plasma exposures were 2- to 3.3-fold higher than the exposures achieved in animals during chronic treatment.

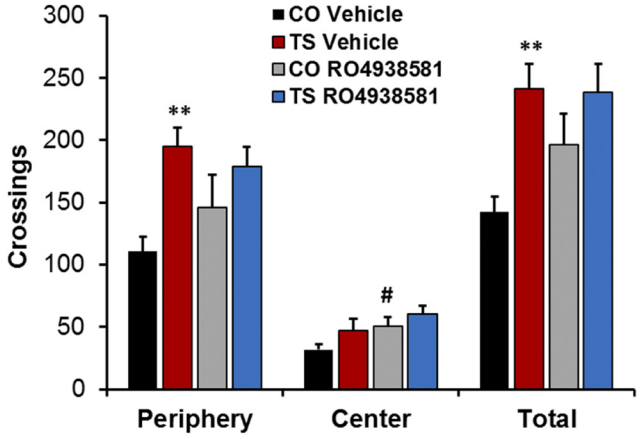

Figure 6. RO4938581 administration did not induce anxiety in the open field. Data are expressed as mean ± SEM of the number of crossings performed by RO4938581- and vehicle-treated TS and CO mice in the center, periphery and of total activity in the open field. $^{**}p < 0.01$, TS versus CO; $^{\#}p < 0.05$, RO498581 versus vehicle; Bonferroni's tests after significant ANOVAs (for statistics, see Table 5).

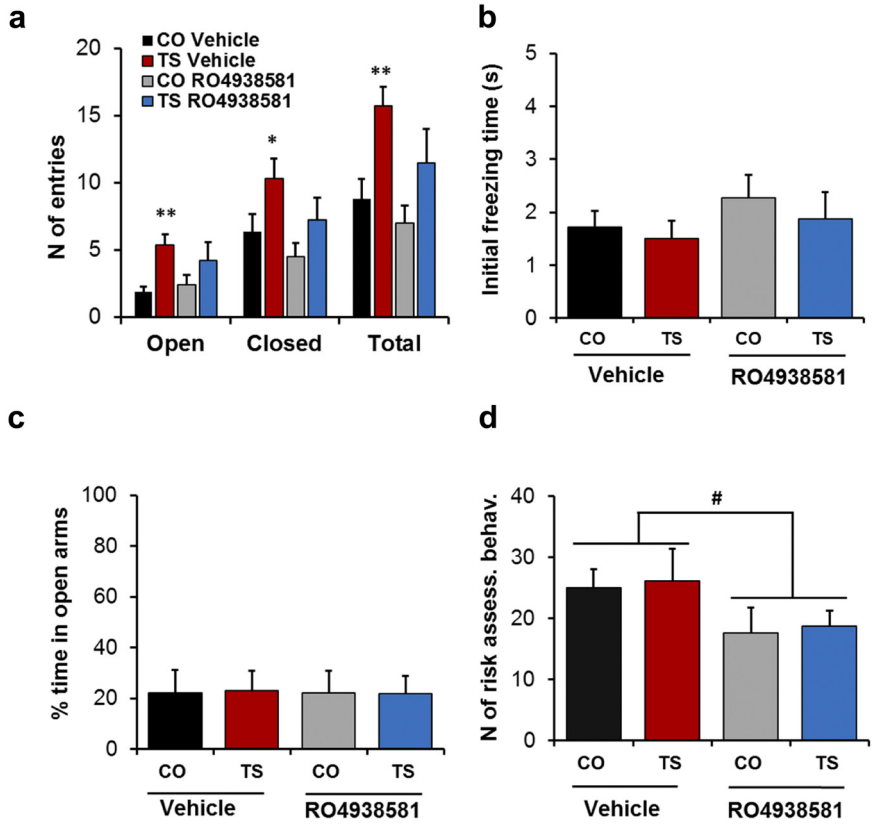

Figure 7. RO4938581 administration reduced hyperactivity of TS mice without inducing anxiety-like behavior in the plus maze. Data are expressed as mean ± SEM of the number of entries in the open and closed arms and number of total entries (***a***), the initial freezing time (***b***), the percentage of time spent in the open arms (***c***), and the number of risk assessment behaviors (***d***) in the plus maze. $^{*}p < 0.05$, $^{**}p < 0.01$, CO versus TS; $^{\#}p < 0.05$, RO498581 versus vehicle; Bonferroni's tests after significant ANOVAs (for statistics, see Table 5).

RO4938581 inhibited *in vivo* binding of [^{3}H]RO0154513 similarly in TS and CO mice

Autoradiographical analysis performed after intravenous injection of the $GABA_A$ α5 subtype preferring radioligand [^{3}H]RO0154513 showed comparable radioligand binding intensities in TS and CO mice, suggesting similar expression levels of $GABA_A$ α5 subunit-containing receptors in both mouse genotypes (Fig. 8*a*, top row). Furthermore, the overall pattern of radioligand binding in the mouse brain was unchanged in both strains and in good agreement with the known distribution of the $GABA_A$ α5 receptor subunit. Strongest staining was observed in brain regions known to contain high densities of $GABA_A$ α5, such as the hippocampus and frontal cortex, whereas regions known to contain less $GABA_A$ α5, such as the striatum and cerebellum, showed lower accumulation of [^{3}H]RO0154513.

The degree of $GABA_A$ α5 occupancy by a dose of 20 mg/kg RO4938581 was estimated by evaluating the ability of the drug to block the *in vivo* binding of [^{3}H]RO0154513. In both TS and CO mice, RO4938581 strongly reduced [^{3}H]RO0154513 signals in hippocampus and frontal cortex (Fig. 8*a*, bottom row). Plasma and brain exposure of 20 mg/kg RO4938581 was found to be similar in both genotypes (mean plasma exposure, 1311 and 1395 ng/ml and mean brain exposure, 905 and 995 ng/ml for CO and TS, respectively). Inhibition of radioligand binding by 20 mg/kg RO4938581 in the hippocampus of TS and CO mice was estimated using the hippocampus/cerebellum ratio of radioligand accumulation as an indication of specific radioligand binding. Pretreatment of TS and CO mice with RO4938581 decreased specific binding of [^{3}H]RO0154513 in the hippocampus by 72 and 68%, respectively (Fig. 8*b*).

Discussion

These results demonstrate that selectively inhibiting the effect of GABA at $GABA_A$ α5 receptors can reverse concomitantly electrophysiological, morphological, and cognitive deficits of TS mice. In this study, we showed that chronic administration of a $GABA_A$ α5 NAM, RO4938581, rescued cognition and behavioral deficits in adult TS mice without inducing anxiety, convulsions, or overt motor effects. In addition, we showed that, in the hippocampus of chronically treated TS mice, RO4938581 rescued the deficits in LTP, adult neurogenesis, and normalized the density of GABAergic synapse markers.

In agreement with previous studies (Escorihuela et al., 1995; Holtzman et al., 1996; Rueda et al., 2008a), TS mice had a pronounced learning deficit in the acquisition sessions of the visible and hidden platform task as well as in the probe trial of the Morris water maze. Chronic treatment with RO4938581 significantly improved TS mice performance in the acquisition sessions, probe trial, and cued sessions, indicating rescue of spatial learning and memory. In addition, vehicle-treated TS mice displayed enhanced thigmotaxis; RO4938581 reduced this behavior in TS and CO mice in the hidden and visible platform tasks of the maze, indicating that drug treatment improved navigation strategies. These results are in agreement with those by Braudeau et al. (2011) who also reported an improvement in spatial learning and navigation strategies in the Morris water maze with another functionally selective $GABA_A$ α5 NAM.

Enhanced thigmotactic behavior of TS mice and their poor performance in the cued test could be related to a profound disruption in procedural learning that was subsequently ameliorated by RO4938581 treatment. It is possible that TS mice have an impaired ability to inhibit an inadequate learning strategy that probably is responsible for the enhanced escape latencies in the water maze. There is evidence that the visible platform task also requires different procedural learning abilities (Whishaw and Mittleman, 1986; Fenton and Bures, 1993). Procedural learning is dependent on striatal function, and it has been shown that the intrastriatal cholinergic system is functionally altered in TS mice (Di Filippo et al., 2010).

In this study, vehicle-treated CO mice performed well in both the acquisition sections and probe trial of the water maze: there was no difference in performance between RO4938581- and vehicle-treated CO mice. This could have been attributable to a "ceiling effect" that resulted in the inability to detect additional improvement in learning and memory after drug treatment in the mice. Alternatively $GABA_A$ $\alpha5$ NAMs may have a selective effect on memory under conditions in which there is excessive inhibition.

Hippocampal-mediated cognitive processes involve long-term changes in synaptic efficacy, such as LTP. Several studies have reported that there is deficient LTP in the hippocampus of TS mice that was pharmacologically rescued by blocking either $GABA_A$ or $GABA_B$ receptors (Kleschevnikov et al., 2004; Costa and Grybko, 2005; Fernandez et al., 2007; Kleschevnikov et al., 2012). In the present study, a more physiologic, theta burst stimulus was used to induce LTP in the CA1 region of the hippocampus. TS mice had an LTP deficit, similar to that reported previously by Costa and Grybko (2005). Chronic treatment with RO4938581 completely rescued the LTP deficit of TS mice and also tended to enhance the induction of LTP in CO mice. Previous studies showed that RO4938581 and other $GABA_A$ $\alpha5$ NAMs enhanced LTP after acute treatment in mouse hippocampal slices (Collinson et al., 2006; Dawson et al., 2006; Ballard et al., 2009). $GABA_A$ $\alpha5$ receptors, predominantly localized extrasynaptically, mediate tonic inhibition (Glykys et al., 2008) and regulate the excitability of hippocampal pyramidal neurons by influencing the strength of depolarization required to generate an action potential (Bonin et al., 2007). Our results provide additional evidence for a major role of $GABA_A$ $\alpha5$ receptors in the modulation of long-term synaptic plasticity and suggest that this may be a mechanism whereby RO4938581 treatment rescues cognitive deficits in TS mice.

In TS mice, deficits in hippocampus-dependent learning and synaptic plasticity have been linked to enhanced inhibition, and these functional deficits seem to correlate with alterations in hippocampal morphology, such as reductions in granule cell density and hippocampal neurogenesis (Insausti et al., 1998; Rueda et al., 2005; Clark et al., 2006; Lorenzi and Reeves, 2006; Bianchi et al., 2010; Llorens-Martín et al., 2010). In agreement with those studies, we found hippocampal neurogenesis and the number of mature granule cells reduced in TS mice. Importantly, chronic administration of RO4938581 fully restored both the density of proliferating cells and the number of mature granule cells in the GCL of TS mice. These results suggest that chronic treatment with RO4938581 can restore cell proliferation and survival of neurons that have undergone maturation in TS mouse hippocampus probably as a consequence of restoring deficient LTP. Indeed, synaptic plasticity within a cellular network of mature hippocampal neurons has been shown to promote neuronal differentiation of newly generated cells (Babu et al., 2009). In addition, $GABA_A$ receptor activity has been shown to regulate neuronal proliferation, migration, differentiation, and integration of newly generated neurons (Tozuka et al., 2005; Ge et al., 2006; Earnheart et al., 2007; Song et al., 2012). Because both newborn and mature neurons seem implicated in hippocampus-dependent learning and memory, the restoration of proliferation and the density of mature neurons is likely to be involved in the cognitive-enhancing effects of RO4938581 in TS mice. A recent study showed that restoring neurogenesis with fluoxetine improved cognitive performance in TS mice (Bianchi et al., 2010).

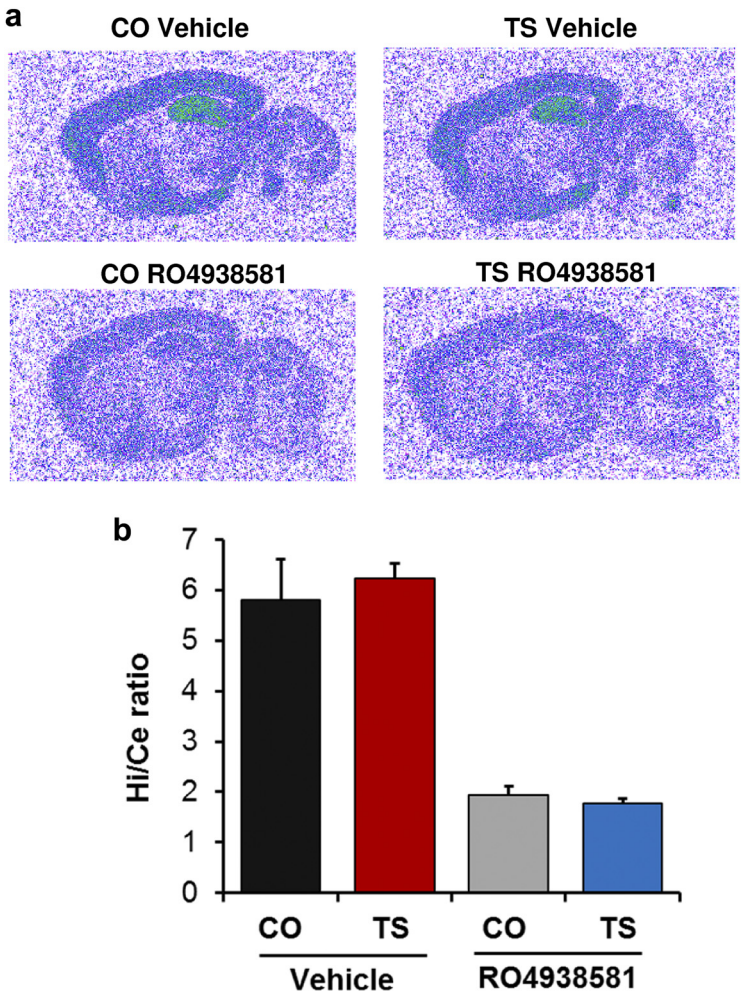

Figure 8. Inhibition of [^{3}H]RO0154513 *in vivo* binding by RO4938581 (20 mg/kg) in TS and CO mice. ***a***, Representative *ex vivo* autoradiographical images of sagittal brain sections of CO and TS mice injected with [^{3}H]RO0154513 and pretreated with vehicle or RO4938581. ***b***, Inhibition of specific radioligand binding by RO4938581 (20 mg/kg) in the hippocampus of CO and TS mice. Data are expressed as the hippocampus/cerebellum ratio of radioligand binding assuming that binding in the cerebellum is mainly nonspecific.

In line with enhanced GABA-mediated inhibition observed in TS mice, we found an increased density of the GABAergic synapse markers GAD65, GAD67, and VGAT in the molecular layer of the hippocampus of TS mice that was normalized by chronic RO4938581 administration. Increased immunoreactivity of proteins associated with GABAergic synapses, including GAD67, VGAT, $GABA_A$ receptor-associated protein, and neuroligin 2, had been measured previously in the neocortex and hippocampus of TS mice (Belichenko et al., 2009; Pérez-Cremades et al., 2010). Because numerous studies have shown that TS mice display morphological and functional alterations in inhibitory circuitries in the hippocampus and cerebral cortex (Belichenko et al., 2004, 2009; Chakrabarti et al., 2010; Pérez-Cremades et al., 2010; Begenisic et al., 2011), it is possible that RO4938581 rescued cognitive deficits in TS mice by normalizing the number and function of inhibitory synapses and, therefore, reestablished circuit inhibitory/excitatory balance and neuroplasticity. In addition, our results suggest that drug treatment in normal animals might induce compensatory mechanisms to maintain circuit inhibitory/excitatory balance in the CNS.

Consistent with previous reports (Escorihuela et al., 1995; Coussons-Read and Crnic, 1996), we also found TS mice hyperactive in the open field, plus maze, and hole-board procedures. Chronic treatment with RO4938581 suppressed hyperactivity in the plus maze and hole board but not in the open field. It has been proposed that the hyperactivity of TS mice in situations that usually provoke caution and suppress activity in normal mice (Escorihuela et al., 1995; Coussons-Read and Crnic, 1996; Martínez-Cué et al., 2006) is attributable to reduced attention to potentially dangerous stimuli (Crnic and Pennington, 2000). Interestingly, RO4938581 also rescued the attention deficits found in TS mice in the hole-board method.

Importantly, RO4938581 did not induce anxiety-like behavior in the open field and plus maze. On the contrary, chronic treatment with this compound had an anti-anxiety-like effect because it increased the number of crossings performed by CO mice in the center of the open field. In the plus maze, although RO4938581 did not affect the motor components of anxiety, it reduced a cognitive component of anxiety as indicated by the lower number of risk assessment behaviors performed by chronically treated TS and CO mice. In addition, RO4938581 did not induce convulsions in TS or CO mice after chronic treatment or when administered at a dose higher than that used in the chronic study. RO4938581 did not modify motor ability, coordination, or amount of spontaneous activity in TS or CO mice. These results further confirm a previous report (Ballard et al., 2009) that showed that RO4938581 did not induce several relevant CNS side effects. In agreement with data on α5IA, a functionally selective $GABA_A$ α5 NAM (Braudeau et al., 2011), our results support the notion that $GABA_A$ α5 receptors may be appropriate drug targets for improving cognition in DS without the unwanted side effects associated with activity at other $GABA_A$ receptor subtypes.

In vivo binding experiments using [^{3}H]RO0154513 demonstrated similar density and distribution of $GABA_A$ α5 receptors in TS and CO mice that is in agreement with mRNA expression data (Vink et al., 2009). Also, similar levels of receptor occupancy were observed in the hippocampus of RO4938581-treated TS and CO mice. Treatment with RO4938581 (20 mg/kg, p.o.) decreased the hippocampal binding of [^{3}H]RO0154513 in both genotypes by ~70%. These data suggest that occupancy and negative modulation of ~70% of hippocampal $GABA_A$ α5 receptors is required for the observed pharmacological effect of RO4938581 in TS mice. Together, these results provide evidence for the potential therapeutic use of selective $GABA_A$ α5 NAMs to treat cognitive deficits in individuals with DS.

References

Babu H, Ramirez-Rodriguez G, Fabel K, Bischofberger J, Kempermann G (2009) Synaptic network activity induces neuronal differentiation of adult hippocampal precursor cells through BDNF signaling. Front Neurosci 3:49. CrossRef Medline

Ballard TM, Knoflach F, Prinssen E, Borroni E, Vivian JA, Basile J, Gasser R, Moreau JL, Wettstein JG, Buettelmann B, Knust H, Thomas AW, Trube G, Hernandez MC (2009) RO4938581, a novel cognitive enhancer acting at $GABA_A$ α5 subunit-containing receptors. Psychopharmacology 202:207–223. CrossRef Medline

Begenisic T, Spolidoro M, Braschi C, Baroncelli L, Milanese M, Pietra G, Fabbri ME, Bonanno G, Cioni G, Maffei L, Sale A (2011) Environmental enrichment decreases GABAergic inhibition and improves cognitive abilities, synaptic plasticity, and visual functions in a mouse model of Down syndrome. Front Cell Neurosci 5:29. CrossRef Medline

Belichenko PV, Masliah E, Kleschevnikov AM, Villar AJ, Epstein CJ, Salehi A, Mobley WC (2004) Synaptic structural abnormalities in the Ts65Dn mouse model of Down Syndrome. J Comp Neurol 480:281–298. CrossRef Medline

Belichenko PV, Kleschevnikov AM, Masliah E, Wu C, Takimoto-Kimura R, Salehi A, Mobley WC (2009) Excitatory-inhibitory relationship in the fascia dentata in the Ts65Dn mouse model of Down syndrome. J Comp Neurol 512:453–466. CrossRef Medline

Bianchi P, Ciani E, Guidi S, Trazzi S, Felice D, Grossi G, Fernandez M, Giuliani A, Calz à L, Bartesaghi R (2010) Early pharmacotherapy restores neurogenesis and cognitive performance in the Ts65Dn mouse model for Down syndrome. J Neurosci 30:8769–8779. CrossRef Medline

Bittles AH, Bower C, Hussain R, Glasson EJ (2007) The four ages of Down syndrome. Eur J Public Health 17:221–225. CrossRef Medline

Bonin RP, Martin LJ, MacDonald JF, Orser BA (2007) α5 $GABA_A$ receptors regulate the intrinsic excitability of mouse hippocampal pyramidal neurons. J Neurophysiol 98:2244–2254. CrossRef Medline

Braudeau J, Delatour B, Duchon A, Pereira PL, Dauphinot L, de Chaumont F, Olivo-Marin JC, Dodd RH, Hérault Y, Potier MC (2011) Specific targeting of the GABA-A receptor α5 subtype by a selective inverse agonist restores cognitive deficits in Down syndrome mice. J Psychopharmacol 25:1030–1042. CrossRef Medline

Chakrabarti L, Best TK, Cramer NP, Carney RS, Isaac JT, Galdzicki Z, Haydar TF (2010) Olig1 and Olig2 triplication causes developmental brain defects in Down syndrome. Nat Neurosci 13:927–934. CrossRef Medline

Clark S, Schwalbe J, Stasko MR, Yarowsky PJ, Costa AC (2006) Fluoxetine rescues deficient neurogenesis in hippocampus of the Ts65Dn mouse model for Down syndrome. Exp Neurol 200:256–261. CrossRef Medline

Collinson N, Kuenzi FM, Jarolimek W, Maubach KA, Cothliff R, Sur C, Smith A, Otu FM, Howell O, Atack JR, McKernan RM, Seabrook GR, Dawson GR, Whiting PJ, Rosahl TW (2002) Enhanced learning and memory and altered GABAergic synaptic transmission in mice lacking the α5 subunit of the $GABA_A$ receptor. J Neurosci 22:5572–5580. Medline

Collinson N, Atack JR, Laughton P, Dawson GR, Stephens DN (2006) An inverse agonist selective for α5 subunit-containing $GABA_A$ receptors improves encoding and recall but not consolidation in the Morris water maze. Psychopharmacology (Berl) 188:619–628. CrossRef Medline

Costa AC, Grybko MJ (2005) Deficits in hippocampal CA1 LTP induced by TBS but not HFS in the Ts65Dn mouse: a model of Down syndrome. Neurosci Lett 382:317–322. CrossRef Medline

Coussons-Read ME, Crnic LS (1996) Behavioral assessment of the Ts65Dn mouse, a model for Down syndrome: altered behavior in the elevated plus maze and open field. Behav Genet 26:7–13. CrossRef Medline

Crestani F, Keist R, Fritschy JM, Benke D, Vogt K, Prut L, Blüthmann H, Möhler H, Rudolph U (2002) Trace fear conditioning involves hippocampal α5 $GABA_A$ receptors. Proc Natl Acad Sci USA 99:8980–8985. CrossRef Medline

Crnic LS, Pennington BF (2000) Down syndrome: neuropsychology and animal models. In: Progress in infancy research (Rovee-Collier C, Lipsitt LP, Hayne H, eds), pp 69–111. Sussex, UK: Psychology Press.

Dawson GR, Maubach KA, Collinson N, Cobain M, Everitt BJ, MacLeod AM, Choudhury HI, McDonald LM, Pillai G, Rycroft W, Smith AJ, Sternfeld F, Tattersall FD, Wafford KA, Reynolds DS, Seabrook GR, Atack JR (2006) An inverse agonist selective for α5 subunit-containing $GABA_A$ receptors

enhances cognition. J Pharmacol Exp Ther 316:1335–1345. CrossRef Medline

Di Filippo M, Tozzi A, Ghiglieri V, Picconi B, Costa C, Cipriani S, Tantucci M, Belcastro V, Calabresi P (2010) Impaired plasticity at specific subset of striatal synapses in the Ts65Dn mouse model of Down syndrome. Biol Psychiatry 67:666–671. CrossRef Medline

Dorow R, Horowski R, Paschelke G, Amin M (1983) Severe anxiety induced by FG 7142, a beta-carboline ligand for benzodiazepine receptors. Lancet 2:98–99. Medline

Earnheart JC, Schweizer C, Crestani F, Iwasato T, Itohara S, Mohler H, Lüscher B (2007) GABAergic control of adult hippocampal neurogenesis in relation to behavior indicative of trait anxiety and depression states. J Neurosci 27:3845–3854. CrossRef Medline

Escorihuela RM, Fernández-Teruel A, Vallina IF, Baamonde C, Lumbreras MA, Dierssen M, Tobeña A, Flórez J (1995) A behavioral assessment of Ts65Dn mice: a putative Down syndrome model. Neurosci Lett 199:143–146. CrossRef Medline

Fenton AA, Bures J (1993) Place navigation in rats with unilateral tetrodotoxin inactivation of the dorsal hippocampus: place but not procedural learning can be lateralized to one hippocampus. Behav Neurosci 107:552–564. CrossRef Medline

Fernandez F, Morishita W, Zuniga E, Nguyen J, Blank M, Malenka RC, Garner CC (2007) Pharmacotherapy for cognitive impairment in a mouse model of Down syndrome. Nat Neurosci 10:411–413. CrossRef Medline

Fritschy JM, Mohler H (1995) $GABA_A$-receptor heterogeneity in the adult rat brain: differential regional and cellular distribution of seven major subunits. J Comp Neurol 359:154–194. CrossRef Medline

Ge S, Goh EL, Sailor KA, Kitabatake Y, Ming GL, Song H (2006) GABA regulates synaptic integration of newly generated neurons in the adult brain. Nature 439:589–593. CrossRef Medline

Glykys J, Mann EO, Mody I (2008) Which $GABA_A$ receptor subunits are necessary for tonic inhibition in the hippocampus? J Neurosci 28: 1421–1426. CrossRef Medline

Holtzman DM, Santucci D, Kilbridge J, Chua-Couzens J, Fontana DJ, Daniels SE, Johnson RM, Chen K, Sun Y, Carlson E, Alleva E, Epstein CJ, Mobley WC (1996) Developmental abnormalities and age-related neurodegeneration in a mouse model of Down syndrome. Proc Natl Acad Sci USA 93:13333–13338. CrossRef Medline

Insausti AM, Megías M, Crespo D, Cruz-Orive LM, Dierssen M, Vallina IF, Insausti R, Floróz J, Vallina TF (1998) Hippocampal volume and neuronal number in Ts65Dn mice: a murine model of Down syndrome. Neurosci Lett 253:175–178. CrossRef Medline

Kahlem P, Sultan M, Herwig R, Steinfath M, Balzereit D, Eppens B, Saran NG, Pletcher MT, South ST, Stetten G, Lehrach H, Reeves RH, Yaspo ML (2004) Transcript level alterations reflect gene dosage effects across multiple tissues in a mouse model of down syndrome. Genome Res 14:1258–1267. CrossRef Medline

Kleschevnikov AM, Belichenko PV, Villar AJ, Epstein CJ, Malenka RC, Mobley WC (2004) Hippocampal long-term potentiation suppressed by increased inhibition in the Ts65Dn mouse, a genetic model of Down syndrome. J Neurosci 24:8153–8160. CrossRef Medline

Kleschevnikov AM, Belichenko PV, Faizi M, Jacobs LF, Htun K, Shamloo M, Mobley WC (2012) Deficits in cognition and synaptic plasticity in a mouse model of Down syndrome ameliorated by $GABA_B$ receptor antagonists. J Neurosci 32:9217–9227. CrossRef Medline

Kurt MA, Davies DC, Kidd M, Dierssen M, Flórez J (2000) Synaptic deficit in the temporal cortex of partial trisomy 16 (Ts65Dn) mice. Brain Res 858:191–197. CrossRef Medline

Kurt MA, Kafa MI, Dierssen M, Davies DC (2004) Deficits of neuronal density in CA1 and synaptic density in the dentate gyrus, CA3 and CA1, in a mouse model of Down syndrome. Brain Res 1022:101–109. CrossRef Medline

Little HJ, Nutt DJ, Taylor SC (1984) Acute and chronic effects of the benzodiazepine receptor ligand FG 7142: proconvulsant properties and kindling. Br J Pharmacol 83:951–958. CrossRef Medline

Liu DP, Schmidt C, Billings T, Davisson MT (2003) Quantitative PCR genotyping assay for the Ts65Dn mouse model of Down syndrome. Biotechniques 35:1170–1174, 1176, 1178 passim.

Llorens-Martín MV, Rueda N, Tejeda GS, Flórez J, Trejo JL, Martínez-Cué C (2010) Effects of voluntary physical exercise on adult hippocampal neurogenesis and behavior of Ts65Dn mice, a model of Down syndrome. Neuroscience 171:1228–1240. CrossRef Medline

Llorens-Martín M, Torres-Alemán I, Trejo JL (2006) Pronounced individual variation in the response to the stimulatory action of exercise on immature hippocampal neurons. Hippocampus 16:480–490. CrossRef Medline

Lorenzi HA, Reeves RH (2006) Hippocampal hypocellularity in the Ts65Dn mouse originates early in development. Brain Res 1104:153–159. CrossRef Medline

Lott IT, Dierssen M (2010) Cognitive deficits and associated neurological complications in individuals with Down's syndrome. Lancet Neurol 9:623–633. CrossRef Medline

Martínez-Cué C, Rueda N, García E, Flórez J (2006) Anxiety and panic responses to a predator in male and female Ts65Dn mice, a model for Down syndrome. Genes Brain Behav 5:413–422. CrossRef Medline

Morris RG, Garrud P, Rawlins JN, O'Keefe J (1982) Place navigation impaired in rats with hippocampal lesions. Nature 297:681–683. CrossRef Medline

Nutt DJ, Besson M, Wilson SJ, Dawson GR, Lingford-Hughes AR (2007) Blockade of alcohol's amnestic activity in humans by an α5 subtype benzodiazepine receptor inverse agonist. Neuropharmacology 53:810–820. CrossRef Medline

Pérez-Cremades D, Hernández S, Blasco-Ibáñez JM, Crespo C, Nacher J, Varea E (2010) Alteration of inhibitory circuits in the somatosensory cortex of Ts65Dn mice, a model for Down's syndrome. J Neural Transm 117:445–455. CrossRef Medline

Reeves RH, Irving NG, Moran TH, Wohn A, Kitt C, Sisodia SS, Schmidt C, Bronson RT, Davisson MT (1995) A mouse model for Down syndrome exhibits learning and behaviour deficits. Nat Genet 11:177–184. CrossRef Medline

Rodgers RJ, Johnson NJ (1995) Factor analysis of spatiotemporal and ethological measures in the murine elevated plus-maze test of anxiety. Pharmacol Biochem Behav 52:297–303. CrossRef Medline

Rudolph U, Knoflach F (2011) Beyond classical benzodiazepines: novel therapeutic potential of $GABA_A$ receptor subtypes. Nat Rev Drug Discov 10:685–697. CrossRef Medline

Rueda N, Mostany R, Pazos A, Flórez J, Martínez-Cué C (2005) Cell proliferation is reduced in the dentate gyrus of aged but not young Ts65Dn mice, a model of Down syndrome. Neurosci Lett 380:197–201. CrossRef Medline

Rueda N, Flórez J, Martínez-Cué C (2008a) Chronic pentylenetetrazole but not donepezil treatment rescues spatial cognition in Ts65Dn mice, a model for Down syndrome. Neurosci Lett 433:22–27. CrossRef Medline

Rueda N, Flórez J, Martínez-Cué C (2008b) Effects of chronic administration of SGS-111 during adulthood and during the pre- and post-natal periods on the cognitive deficits of Ts65Dn mice, a model of Down syndrome. Behav Brain Res 188:355–367. CrossRef Medline

Siarey RJ, Stoll J, Rapoport SI, Galdzicki Z (1997) Altered long-term potentiation in the young and old Ts65Dn mouse, a model for Down Syndrome. Neuropharmacology 36:1549–1554. CrossRef Medline

Song J, Zhong C, Bonaguidi MA, Sun GJ, Hsu D, Gu Y, Meletis K, Huang ZJ, Ge S, Enikolopov G, Deisseroth K, Luscher B, Christian KM, Ming GL, Song H (2012) Neuronal circuitry mechanism regulating adult quiescent neural stem-cell fate decision. Nature 489:150–154. CrossRef Medline

Stasko MR, Costa AC (2004) Experimental parameters affecting the Morris water maze performance of a mouse model of Down syndrome. Behav Brain Res 154:1–17. CrossRef Medline

Tozuka Y, Fukuda S, Namba T, Seki T, Hisatsune T (2005) GABAergic excitation promotes neuronal differentiation in adult hippocampal progenitor cells. Neuron 47:803–815. CrossRef Medline

Vink J, Incerti M, Toso L, Roberson R, Abebe D, Spong CY (2009) Prenatal NAP+SAL prevents developmental delay in a mouse model of Down syndrome through effects on *N*-methyl-D-aspartic acid and gamma-aminobutyric acid receptors. Am J Obstet Gynecol 200:524.e1–e4. CrossRef Medline

Whishaw IQ, Mittleman G (1986) Visits to starts, routes, and places by rats (*Rattus norvegicus*) in swimming pool navigation tasks. J Comp Psychol 100:422–431. CrossRef Medline